



Research paper

Analysis of nuclear-renewable hybrid energy system for marine ships

Hossam A. Gabbar ^{a,b,*}, Md. Ibrahim Adham ^a, Muhammad R. Abdussami ^a^a Faculty of Energy Systems and Nuclear Science, Ontario Tech University (UOIT), 2000 Simcoe St N, Oshawa ON L1G 0C5, Canada^b Faculty of Engineering and Applied Science, Ontario Tech University (UOIT), 2000 Simcoe St N, Oshawa ON L1G 0C5, Canada

ARTICLE INFO

Article history:

Received 20 October 2020

Received in revised form 10 April 2021

Accepted 16 April 2021

Available online xxxx

Keywords:

Nuclear power plant

Renewable energy

Hybrid energy systems

Marine ships

ABSTRACT

While several actions are being taken to reduce Greenhouse Gas (GHG) emissions from land-based transportation, marine transportations are often unnoticed. Ocean-going marine ships are accounted for a large amount of global GHG emissions. Renewable Energy Sources (RESs) are free from GHG emissions and playing an important role in sustainable development by lessening GHG emissions. Integration of RESs in ocean-going marine ships could be an option to make marine transportation free from emissions. Ocean-going marine ships require a large amount of reliable energy to support the propulsive load demand. RESs are intermittent, and a large amount of energy cannot be stored economically by the available energy storage techniques. Additionally, the penetration of RESs in a marine ship is limited by the available area and total weight carrying capacity of that marine ship. Because of these limitations of RESs in marine ships, there is a requirement of integrating other types of energy sources with RESs to support the baseload energy demand and to avoid the variableness of RESs. Conventional fossil fuel-based generators, like diesel generators, can be incorporated with RESs to overcome these shortcomings of RESs. However, as the penetration of RESs is limited to marine ships, most of the energy is supplied by fossil fuel-based generators. Therefore, the integration of RESs with fossil fuel-based generators merely reduces GHG emissions and is not a feasible option to make marine ships free from emissions. Fossil fuel-based generators need to be replaced by emissions-free and reliable energy sources to make the marine ships free from emissions. Small scale nuclear reactors, such as Small Modular Reactors (SMRs) and Microreactors (MRs), are free from GHG emissions and are competitive candidates to replace fossil fuel-based generators. In this paper, four different energy systems have been analyzed for marine ships namely 'Stand-alone Fossil Fuel-based Energy System', 'Stand-alone Nuclear Energy System', 'Renewable and Fossil Fuel-based Hybrid Energy System' and 'Nuclear-Renewable Hybrid Energy System (N-R HES)' in terms of certain Key Performance Indicators (KPIs). The KPIs include the Cost of Energy (COE), Net Present Cost (NPC), and GHG emissions. The results show that the N-R HES could be the best energy system for the marine industry to reduce GHG emissions and improve economic performance. A sensitivity analysis is also carried out by changing certain parameters to reinforce the findings of this study.

© 2021 Published by Elsevier Ltd. This is an open access article under the CC BY-NC-ND license (<http://creativecommons.org/licenses/by-nc-nd/4.0/>).

1. Introduction

Reduction of GHG emissions is the main objective to avoid the negative impact of climate change. The target of the Kyoto protocol was to reduce GHG emissions by around 5%, on average, relative to 1990 levels by 2012. International shipping was not included in Paris Agreement but it is responsible for global GHG emissions to a large extent. If global shipping were a country, it would be considered as the sixth-largest producer of GHG emissions. Ocean-going shipping is responsible for more than 3% of global GHG emissions ([Shipping Pollution, 2020](#)). In the

EU countries, water transportation is the second-largest contributor of CO₂ emissions after road transportation ([Anon, 2020a](#)). Emissions from ocean-going ships are almost twice the emissions from total registered cars in the US. Fifteen largest ships emit as much SOx as the world's total of 760 million cars ([Helms, 2020](#)). The Marine Environment Protection Committee (MEPC) of the International Maritime Organization (IMO) set a target in April 2018 to reduce GHG emissions by at least 50% by 2050 compared to 2008 ([Anon, 2020](#)). To reduce GHG emissions, increasing the energy efficiency of marine ships and innovation are two prime requirements. IMO has set a target to increase energy efficiency by 30% within 2025. Several studies have been carried out to improve the energy efficiency of marine ships, such as the identification of optimal trim configurations ([Perera et al., 2015](#)) and

* Corresponding author at: Faculty of Energy Systems and Nuclear Science, Ontario Tech University (UOIT), 2000 Simcoe St N, Oshawa ON L1G 0C5, Canada.

E-mail address: hossam.gaber@ontariotechu.ca (H.A. Gabbar).

Nomenclature		$BAT_{out}(t)$	Amount of energy that is needed from the battery at time step t
AIS	Automatic Identification System	C_{UCH}	UCH emissions penalty (\$/ton)
COE	Cost of Energy	C_{SO_2}	SO ₂ emissions penalty (\$/ton)
CO ₂	Carbon Dioxide	M_{CO_2}	CO ₂ annual emissions (kg/year)
CO	Carbon Monoxide	M_{UCH}	UCH annual emissions (kg/year)
ESS	Energy Storage System	M_{SO_2}	SO ₂ annual emissions (kg/year)
EU	European Union	$P_{L(t)}$	The total demand of load at time t (kW)
FFG	Fossil Fuel-based Generator	$P_{RES(t)}$	Total available power from RESs at time t (kW)
GHG	Greenhouse Gas	$P_{GEN(t)}$	Total available power from generator at time t (kW)
HOMER	Hybrid Optimization of Multiple Energy Resources	$P_{BAT(t)}$	Total available power from battery at time t (kW)
HES	Hybrid Energy System		
IAEA	International Atomic Energy Agency		
ITTC	International Towing Tank Conference		
IMO	International Maritime Organization		
kn	knot		
KN	Kilo Newton		
kg	Kilogram		
kW	Kilowatt		
KPI	Key Performance Indicator		
MW	Megawatt		
L	Liter		
MR	Microreactor		
MEPC	Marine Environment Protection Committee		
NPV	Net Present Value		
NPC	Net Present Cost		
NASA	National Aeronautics and Space Administration		
N-R HES	Nuclear-Renewable Hybrid Energy System		
PV	Photovoltaic		
RES	Renewable Energy Source		
SOC	State of Charge		
SOC _{max}	State of Charge (maximum)		
SO ₂	Sulfur Dioxide		
SOC _{min}	State of charge (minimum)		
SMR	Small Modular Reactor		
TRISO	TRI-structural ISOtropic		
UHC	Unburned Hydrocarbons		
W	Watt		
Variables and Parameters			
$BAT_{chrg}(t)$	Capacity of battery after charging at time step t		
$BAT_{dischrg}(t)$	Capacity of battery after discharging at time step t		
C_{CO}	CO emissions penalty (\$/ton)		
C_{PM}	PM emissions penalty (\$/ton)		
C_{CO_2}	CO ₂ emissions penalty (\$/ton)		
C_{NOx}	NO _x emissions penalty [\$/t]		
M_{CO}	CO annual emissions (kg/year)		
M_{PM}	PM annual emissions (kg/year)		
M_{NOx}	NO _x annual emissions (kg/year)		
$P_{MR(t)}$	Total available power from MR at time t (kW)		
$SOC_{(t)}$	Available SOC of ESS at time t (%)		
$BAT_{in}(t)$	Amount of energy that can be given to the battery at time step t		

up to 10% reduction of fuel consumption by optimizing ship operation (Ang et al., 2000). Several innovative approaches have been taken to reduce the GHG emissions from marine ships, and the introduction of renewable energy in marine ships is one of them. To reduce emissions and increase the efficiency of marine ship operation, renewable energy such as wind energy, biofuels, solar energy, Liquified Natural Gas (LNG) can be introduced in marine ships (Paulson and Chacko, 2019). The energy requirement of ocean-going marine ships is high, and they need a reliable source of energy. Intermittency is one of the limitations of RESs. Electric energy storage systems for an extended period of time are also not economically viable. Additionally, the penetration of RESs in a marine ship is limited by the available area and total weight carrying capacity of that marine ship. To address these issues, other types of energy sources need to be integrated with renewable energy to provide a resilient energy infrastructure. Hence, the integration of RESs with conventional fossil fuel-based energy sources in marine ships has been studied. The combination of RESs with fossil fuel may reduce GHG emissions to a certain extent but it is not completely free from GHG emissions. To make GHG emissions-free marine ship, fossil fuel-based generator needs to be replaced by emissions-free energy sources that can provide reliable power and can assure continuity and resiliency. SMRs and MRs are small-scale fourth-generation nuclear reactors, and it can supply power with essentially zero carbon emissions. Currently, more than fifty SMR designs under development, and six of them are targeted for marine-based applications (Anon, 2018a).

Nuclear-renewable hybrid energy system for ocean-going marine ships has not been discussed and analyzed extensively yet. However, a few studies have been carried out on the stand-alone nuclear energy system and fossil fuel-renewable hybrid energy system in marine ships.

Wen et al. (2017) studied the economic advantages of introducing renewable energy in marine ships. They considered a hybrid energy system, comprising solar PV, wind power generation, ESS, and diesel generator. They analyzed three different cases of energy systems of an oil tanker namely, 'Only Diesel Generator', 'Diesel Generator and Renewable Energy', and 'Diesel Generator, Renewable Energy and ESS'. This study shows that 'Diesel Generator, Renewable Energy and ESS' is economically more feasible than the other two energy systems and has the lowest CO₂ emissions among the three cases. However, the amount of CO₂ emissions from the optimized energy system is significant due to the presence of fossil fuel-based generator.

Techno-economic analysis of integrated PV systems with diesel generator into marine ships has been done by Qiu et al.

(0000). In this case study, they considered six different navigation routes namely 'Asia-Buka-Australia', 'Asia-Bering-Europe', 'Asia-Malacca-Gibraltar-Europe', 'Asia-Panama-Europe', 'Europe-America', and 'Europe-Cape Town-Australia'. They compared the navigation routes in terms of Net Present Value (NPV), Internal Rate of Return (IRR), Levelized Cost of Energy (LCOE), etc. This study indicates that the hybrid PV-Diesel power system for the marine ship is financially feasible. Also, the authors marked the 'Asia-Malacca-Gibraltar-Europe' navigation route as the most feasible route among all the six routes for the hybrid energy system.

Diab et al. (2016) compared hybrid energy systems for marine ships and land-based systems. They took a route from Dalian in China to Aden in Yemen of an oil tanker. In the hybrid renewable energy systems, the authors considered two diesel generators and solar PV. They considered the same electrical demand for both ship and land-based systems. The authors calculated the average solar radiation of six stoppages in the ship navigation route, and the same solar radiation was considered for the land-based system. For the land-based system, the authors did not consider any limitation for solar PV system capacity but for the ship, and they limited the solar PV system to 300 kW considering the usable area of that ship. They analyzed four combinations namely 'Only Diesel Generator', 'Diesel Generator and Battery', 'Diesel Generator and Solar PV System', and 'Diesel Generator, Solar PV System, and Battery'. For 'Only Diesel Generator' and 'Diesel Generator and Battery', there was no difference between the ship and the land-based system in terms of COE, NPC, and GHG emissions. The authors suggested that 'Diesel Generator, Solar PV system, and Battery' could be the optimal solution for both ship and land-based systems although GHG emissions were around nine times higher in ship compared to the land-based system due to the low penetration of PV systems in the ship.

Optimal sizing of solar PV, diesel generator, and battery ESS in an oil tanker was studied in **Lan et al. (2015)**. The authors considered four different cases for economic analysis namely 'cost analysis for diesel generator only', 'cost analysis for diesel generator and solar PV', 'cost analysis for diesel generator, solar PV, and EES', and 'cost analysis considering multi-objective optimization for diesel generator, solar PV, ESS, and CO₂ emissions'. They showed that the Net Present Cost (NPC) and CO₂ emissions of the optimized hybrid energy systems were the lowest among all the energy systems.

Feasibility analysis on a pure battery-electric propulsion system for large ocean-going ships was carried out in **Anon (0000a)**. The paper analyzed three different sizes of container ships, four different sizes of bulk carriers, and one large ro-ro ship. This study suggests that a battery-powered energy system is feasible only for a short distance of a ro-ro ship. This paper also concludes that pure battery-electric propulsion is not feasible for long-distance voyage due to battery weight and volume.

A review of the past work and recent development in the area of nuclear powered ocean-going marine ships was studied in **Hirdaris et al. (2014)**. The authors proposed a concept design of a cargo ship, powered by a 25 MWe SMR. They also studied the associated risk with different power train systems and SMR locations. The authors suggested that SMR location would be preferred at the aft of the cargo tank.

Carlton et al. (2011) summarized nuclear physics and discussed nuclear plants for marine ship considering reactor control, reliability, location of the plant in the ship, protection of reactor, irradiation effect on structural steel of the ship, refueling, and radiation hazard area. They also studied the application of nuclear plant on different marine ships. They considered tankers, container ships, and cruise ships. For each type of ship, they took two sizes – one is a larger size and another is a conventional size. This

study concludes that there is no technological ground that can prevent the use of nuclear energy in merchant ships. However, the authors emphasized altering the general arrangement of ships to provide the best possible operating environment to the reactor. They also emphasized designing the structure of the ship to distribute and absorb the energy of impact and make the ship safe from vibration and collision.

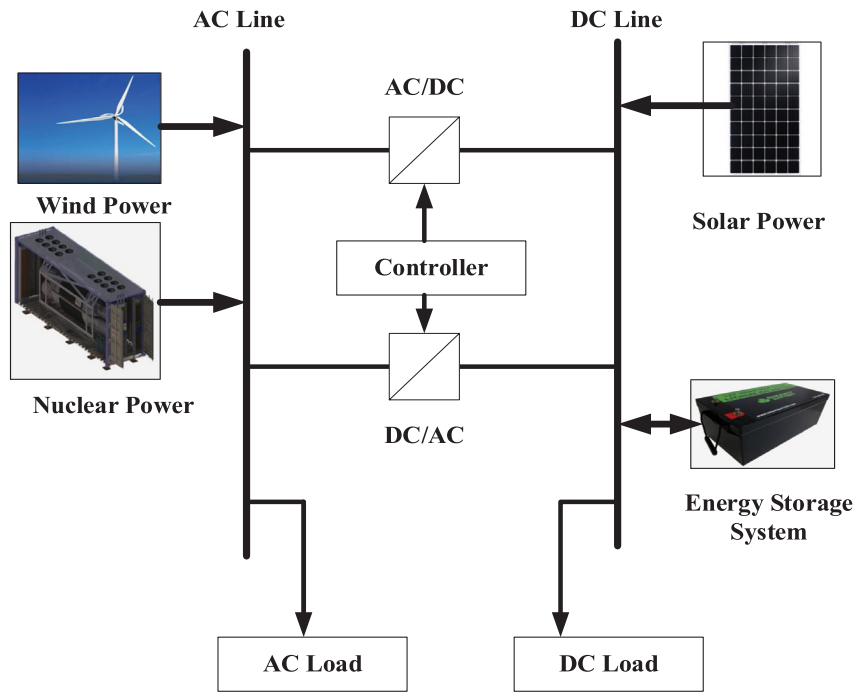
After getting inquiries from Murmansk Shipping Company, HBR (Haven Bedrijf Rotterdam; Harbor Company Rotterdam) researched the cost of getting a permit to enter into the port for 'Sevmorput' – a nuclear-powered ship. It investigated the route between Rotterdam and the Far East. This study concluded that it would cost at least €522,000 for a single permit without considering political disinclination and other policies (**JACOBS, 2007**).

Gravina et al. (2012) addressed two important flaws of nuclear-powered containership, which are route restrictions to enter some national territorial waters and the risk of accident with severe consequences. They proposed a conceptual design of a nuclear-powered containership that could operate freely without any objection from the port states and could withstand any accident without any catastrophic consequences. This study suggests a modular containership with two modules, one is a propulsion module and the other one is a cargo module. The propulsion module contains the nuclear plant whereas the cargo module carries the payload. These two modules can be disjoined before entering into national territorial waters. The propulsion module remains in international waters, and the cargo module enters into national territorial water with the help of any secondary propulsion system. The authors analyzed five different modular nuclear containership concepts and concluded that the tug/barge system could be the best concept based on subjective analysis. To avoid any catastrophic incident resulted from an accident, they suggested strengthening the reactor compartment by cutting decks technology or providing 'Y' shaped frames consisting of sandwich material.

In this paper, an oil tanker, named 'Baltic Sunrise' is considered. It starts from Iraq and stops in Singapore via Egypt and Netherland (Rotterdam). Four different cases are studied and assessed by HOMER software. A comparison is made among all the cases based on three important KPIs – COE, NPC, and GHG emissions. The energy requirement of the oil tanker is estimated based on actual voyage data provided by 'FleetMon'. Also, the GHG emissions penalty is considered in this paper. Sensitivity analysis is conducted to see the impact of different parameters before giving any concluding remark. This document is outlined as follows: system configuration is discussed in Section 2. Design consideration is addressed in Section 3. Section 4 is all about the simulation of four cases. Section 5 covers the simulation result, sensitivity analysis, and comparison among the four cases. Conclusion and future works are discussed in Section 6.

2. System configuration

Fig. 1 shows the proposed N-R HES for a marine ship consisting of MRs, solar PV panels, wind turbines, energy storage systems, controllers, AC/DC converters, and DC/AC converters. Oil tanker 'Baltic Sunrise' is considered in this case study. A vessel data collection company 'FleetMon' provided the AIS data of the ship (**Anon, 2020b**). The energy demand of the ship is estimated based on speed, breadth, draught, frictional resistance, residual resistance, and using the ITTC-57 method and Gertler Series Data chart. Details of the ship's energy demand estimation, system components, and associated assumptions are discussed in the subsections. Some specific KPIs – Net Present Cost (NPC), Cost of Energy (COE), and Greenhouse Gas (GHG) emissions are assessed in this study. HOMER Pro software is used for simulations, system modeling, and KPI analysis. The project lifetime of

**Fig. 1.** Proposed N-R HES for marine ship.

the system is assumed as 40 years. Discount rate, Inflation rate, and Annual capacity shortage are considered as 8%, 2%, and 0%, respectively. Data of solar radiation and wind speed are assumed to be the same for the whole 40 years. In general, equipment efficiency and equipment cost change every year, and to address this issue an additional study is done by the 'Multiyear Analysis' module of HOMER Pro software. The rating of system components is obtained from the HOMER optimizer. HOMER uses two types of optimization, which are original grid search optimization and proprietary derivative-free optimization. In the original grid search optimization, suitable system configuration needs to be defined in the search space and HOMER searches the least-cost combination of equipment with meeting the electric load. In derivative-free optimization, users need not to give any input in the search space, while HOMER finds the optimized rating of the system components. Understanding the electric load and cost information of the system component is needed in derivative-free optimization (Anon, 2020c). In this study, the rating of the system components is obtained by the combination of both optimization techniques. After getting the rating of the system components, a 'Multiyear Analysis' is carried out.

2.1. Ship and route description

In this case study, 'Baltic Sunrise' is taken as a reference marine ship. The IMO number of this ship is 9307633. Detailed parameters of this ship are shown in Table 1.

In this study, the route of Baltic Sunrise is considered for three months from 1st May'19 to 31st July'19. 'Baltic Sunrise' started from Al Basrah Oil Terminal (Iraq) and ended in Pulau Bukom (Singapore). In its' route, it stopped in Ain Shukna (Egypt), Sidi Kirayr (Egypt), and Rotterdam Maashaven (Netherlands).

The speed of this marine ship is different in different positions. The route along with the speed of the 'Baltic Sunrise' is shown in Fig. 2. The figure is created from the data that is provided by FleetMon and plotted in google map.

2.2. Estimation of effective ship power

To solve the real-world problem, practical data is needed. Hourly power requirement data of ship is not readily available. For optimal system design, the detailed power requirement of a ship plays an important role. Hence, estimating the effective power is necessary. In this section effective power of 'Baltic Sunrise' is estimated based on speed, breadth, draught, frictional resistance, residual resistance, and using the ITTC-57 method and Gertler Series Data chart. Seawater temperature is considered as 30 °C in this calculation. Parameters and assumptions that have been considered in this calculation are summarized in Table 2.

To calculate the effective power of a ship, the hull resistance of the ship needs to be calculated. Hull resistance is the addition of residuary resistance and frictional resistance of the ship. After getting the total hull resistance, the effective power of the ship can be calculated by the following equation (Chuku et al., 2017).

$$P_{ship(x,y)} = R_{TBHS} \cdot V_{s(x,y)} \quad (1)$$

where, $P_{ship(x,y)}$ is the effective power of the ship in a certain position (x,y) , R_{TBHS} is the total bare hull resistance of the ship, and $V_{s(x,y)}$ is the speed of the ship in a certain position (x,y) .

The total hull resistance of a ship can be calculated as per the following formula (Chuku et al., 2017).

$$R_{TBHS} = C_{TBHS} \cdot \frac{1}{2} \rho_w \cdot s_s \cdot V_{s_avg}^2 \quad (2)$$

where, R_{TBHS} , C_{TBHS} , ρ_w , s_s , and V_{s_avg} represent the total hull resistance of ship, total hull resistance coefficient of ship, water density, ship surface wetted, and average speed of the ship, respectively.

The total hull resistance coefficient can be calculated as follows (Anon, 2021).

$$C_{TBHS} = C_{fs} + C_{rs} + C_A \quad (3)$$

where, C_{TBHS} , C_{fs} , and C_{rs} denote the total hull resistance coefficient, coefficient of frictional resistance, and the coefficient of residual resistance.

Table 1
Description of Baltic Sunrise (Anon, 2020d).

Sl. no	Ship description
1	Ship's name (IMO number)
2	Date delivered/Builder (where built)
3	Flag/Port of Registry
4	Call sign
5	Type of ship
6	Length overall (LOA)
7	Length between perpendiculars (LBP)
8	Extreme breadth (Beam)
9	Deadweight
10	Displacement



Fig. 2. Route and speed (kn) of 'Baltic Sunrise'.

Table 2
Parameters/assumption of 'Baltic Sunrise'.

Sl. no	Parameter/Assumption	Category	Notation	Value	Reference
1	Beam of the ship	Parameter	B	60 m	Anon (2020d)
2	Volume displacement of the ship	Parameter	v	344649.08 m ³	Anon (2020d)
3	Draught of the ship	Parameter	D	21.6 m	Anon (2020e)
4	Extreme breadth (Beam)	Parameter	B_{ex}	60.04 m	Anon (2020d)
5	Average draught of the ship	Parameter	D_{avg}	16.15 m	Anon (2020e)
6	Length between perpendiculars	Parameter	LBP	324 m	Anon (2020d)
7	Gravitational acceleration	Parameter	g	9.81 m/s ²	
8	Seawater density at 30 °C temperature	Parameter	ρ_w	1021.7 kg/m ³	Chuku et al. (2017)
9	Seawater viscosity at 30 °C temperature	Parameter	γ_w	0.84931 × 10 ⁻⁶ m ³ s ⁻¹	Chuku et al. (2017)
10	Average speed of the ship	Parameter	V_s_{avg}	11.94 kn or 6.1424 ms ⁻¹	Anon (2020e)
11	Incremental resistance coefficient due to surface roughness of ship	Assumption	C_A	0.0004	Chuku et al. (2017)
12	Maximum speed of the ship	Parameter	V_s_{max}	17.9 kn or 9.2185 ms ⁻¹	Anon (2020e)

The waterline length, wetted surface, Reynolds number, coefficient of frictional resistance, and Froude number of the ship can be calculated from the Eqs. (4), (5), (6), (7), and (8), respectively (Chuku et al., 2017; Anon, 2021).

$$L_{wl} = \frac{LBP}{0.97} = 334.02 \text{ m} \quad (4)$$

$$S_s = 1 \cdot 7L_{wl} \cdot B + \frac{v}{D} = 55410.6 \text{ m}^2 \quad (5)$$

$$R_{ns} = \frac{V_s_{avg} \times L_{wl}}{\gamma_w} = 2.42 \times 10^9 \quad (6)$$

$$C_F = \frac{0.075}{(\log R_{ns} - 2)^2} = 1.37 \times 10^{-3} \quad (7)$$

$$F_{ns} = \frac{V_s_{max}}{\sqrt{g \times L_{wl}}} = 0.16 \quad (8)$$

where L_{wl} , R_{ns} , C_F , and F_{ns} denotes waterline length, Reynolds number, coefficient of frictional resistance, and Froude number of 'Baltic Sunrise'.

The ratio of volume displacement to length and beam to draught can be obtained from Eqs. (9) and (10), respectively.

$$\frac{v}{L_{wl}^3} = 9.2 \times 10^{-3} \quad (9)$$

$$\frac{B}{D} \cong 3.00 \quad (10)$$

Midship section area can be found by using the following equation.

$$A_m = B_{ex} \times D_{avg} = 969.646 \text{ m}^2 \quad (11)$$

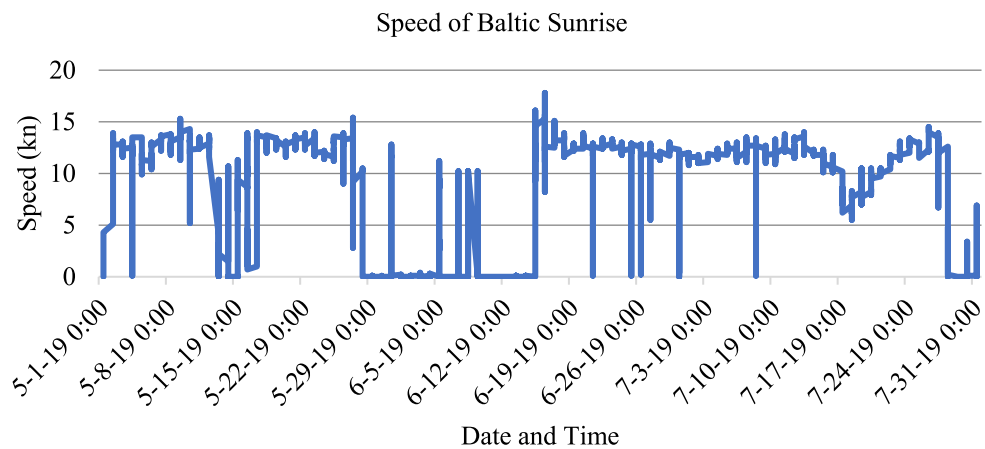


Fig. 3. Speed of Baltic Sunrise (1st May'19 to 31st July'19).

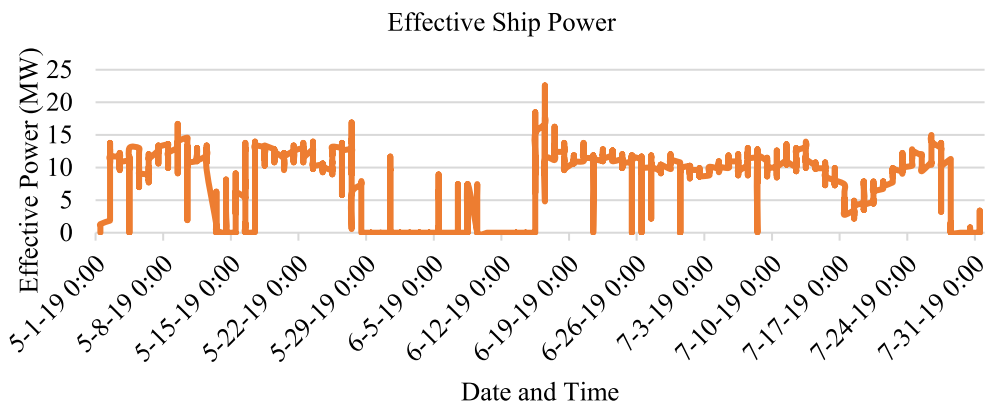


Fig. 4. Estimated effective Power (MW) of Baltic Sunrise (1st May'19 to 31st July'19).

where, A_m is the midship section of the ship. Longitudinal prismatic coefficient (C_p) can be calculated by the following equation.

$$C_p = \frac{v}{A_m L_w} \cong 0.6 \quad (12)$$

Based on Beam to Draught ratio and C_p , the Gertler series is chosen accordingly. From the value of F_{ns} and volume displacement to length ratio, C_{Rs} can be found as 0.75×10^{-3} (Molland et al., 2000).

From Eqs. (2) and (3), C_{TBHS} and R_{TBHS} can be calculated as 0.00252 and 2691.306 KN, respectively.

Now, from Eq. (1), ship effective power can be calculated for different ship speeds in different positions. More details of this calculation can be found in Chuku et al. (2017) and Molland et al. (2000).

Fig. 3. shows the hourly speed of the ship over the 3 months and Fig. 4 shows the hourly estimated effective power or propulsive power of the ship. From the calculation, the maximum ship propulsive power is around 22 MW without considering the auxiliary power requirement.

These three months data are converted to twelve months data in HOMER by replicating the data in the opposite direction, signifying, the first three months data refers to the power requirement when the ship goes from Iraq to Singapore, 2nd three months data refers to the power requirement from Singapore to Iraq, 3rd three months data is from Iraq to Singapore, and last three months data is from Singapore to Iraq.

In this study, along with the 'Ship Propulsive Power Load', two other types of electrical loads are added. The first one is 'Auxiliary Load' to emulate the electrical load demand for cooling, light, feed

systems, pumps, air compressors, distillation equipment, etc. The second load is a 'Deferrable Load' to add diversity in the load, which will get less priority compared to 'Ship Propulsive Power Load' and 'Auxiliary Load'. In the simulation, energy resources supply electricity to 'Ship Propulsive Power Load' and 'Auxiliary Load' first and then go for 'Deferrable Load'. Electrical loads are summarized in Table 3. Fig. 5. shows the yearly propulsive electric load in the one-hour interval.

2.3. Diesel generator

FFG is not mandatory for N-R HESs in marine ships. However, to compare the proposed N-R HES with the traditional energy system, a diesel Genset is considered here. In the conventional energy system of marine ships, there is a diesel generator along with small scale energy storage systems. The traditional hybrid energy system in marine ships consists of FFGs, RESs, power converters, and energy storage systems. In this study, the rating of the smallest unit of diesel generator and MR is 1 MW since both of the energy resources have modularity features. Diesel price is considered as 0.639 UDS/Liter (Anon, 2020f). Economic Parameters of the diesel generator are summarized in Table 5. Total emissions by the diesel generator are calculated by the HOMER software.

2.4. Solar power

For converting solar radiation to useful electricity, Solar PV systems are used in this study. Solar radiation changes in the navigation route with longitude and latitude, time, date, etc. For

Table 3
Specifications of propulsive and auxiliary electric load.

Parameter	Value	
	Propulsive electric load	Auxiliary electric load
Average energy demand (kWh/day)	176,057.04	23,997.64
Average power demand (kW)	7,335.71	999.07
Peak power demand (kW)	22,600.96	2093.1
Load factor (%)	0.32	0.48

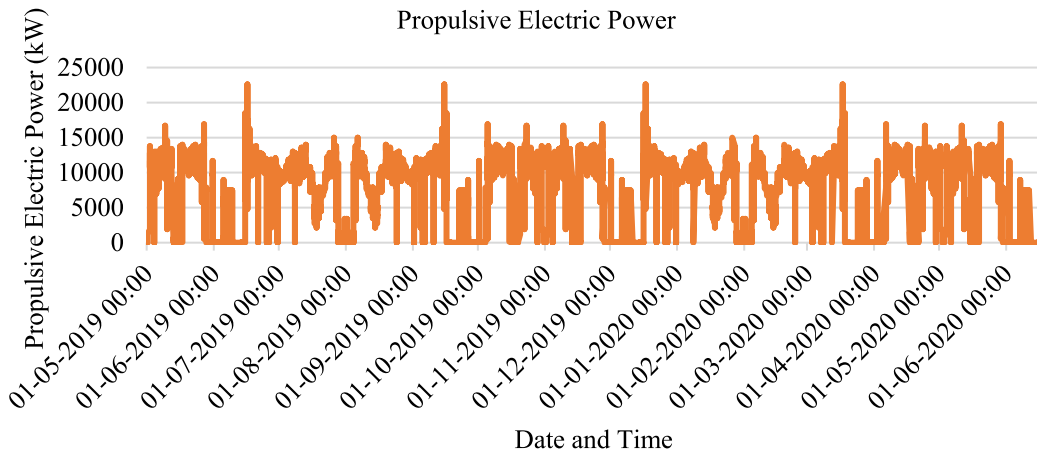


Fig. 5. Hourly propulsive electric load for 1st year of project life.

the sake of simple calculation, the average solar radiation of the five stoppage ports is considered in this study. The solar radiation data of these five ports are collected from the NASA Surface meteorology and Solar Energy database. The average monthly solar radiation of five ports is presented in Fig. 6. The average solar radiation of all five ports is also presented in the same figure. GPS and annual average solar radiation of five ports are summarized in Table 4. It is assumed that annual solar radiation will be the same throughout the project lifetime.

Unlike a land-based energy system, there is a limitation to use solar PV systems in marine ships because of the limited space. In this study, 'Baltic Sunrise', a crude oil tanker is considered having a length and width of 333.12 m and 60.04 m, respectively. Therefore, theoretically, the maximum allowable area that can be used for the solar PV system is 20000.52 m².

There are two common configurations for solar panels, which are 60-cell and 72-cell. 60-cell solar panels range from 285 W to 315 W, and 72-cell solar panels range from 335 W to 375 W. For a 6.5 kW system, 18 panels of the 72-cell solar panel are required (Anon, 0000b). The length and width of each 72-cell solar panel are 77 inches and 36 inches, respectively. Hence, the maximum allowable solar PV system that can be installed on the ship is 4038 kW. In practice, the total ship space cannot be used for solar PV and some space will be required by the wind turbine. Hence, 40% of the maximum allowable solar PV system is considered in this study, which is around 1600 kW.

The output power of the solar PV can be calculated by the following equation (Anon, 0000c).

$$P_{PV} = Y_{PV} f_{PV} \left(\frac{G_T}{G_{T,STC}} \right) [1 + \alpha_p (T_c - T_{c,STC})] \quad (13)$$

where, Y_{PV} , f_{PV} , G_T , $G_{T,STC}$, α_p , T_c , and $T_{c,STC}$ refer rated capacity of the PV array under standard test conditions (kW), derating factor of PV (%), Solar radiation incident on PV in the current time step (kW/m²), solar incident radiation at standard test condition (1 kW/m²), coefficient of temperature (%/°C), the temperature of PV cell in the current time step (°C), and temperature of PV cell under standard test conditions (25°C), respectively.

"Standard Test Condition (STC)" denotes the PV power rating at a specific condition set by the manufacturers. Solar radiation and temperature of a solar cell, are assumed to be 1 kW/m² and 25°C, respectively in STC. Also, no flow of wind is considered around the PV cell in STC. However, in general, the temperature of the full-sun cell is always greater than 25°C and wind always flows around the PV cell. The derating factor is related to wiring losses, panel losses, and aging. To match the manufacturer's rating of the solar PV with actual conditions, the derating factor is used. Parameters of solar PV are summarized in Table 5.

Eq. (13) can be simplified as follows by ignoring the temperature effect.

$$P_{PV} = Y_{PV} f_{PV} \left(\frac{G_T}{G_{T,STC}} \right) \quad (14)$$

2.5. Wind power

In HOMER, the output power of a wind turbine is calculated by three steps (Anon, 0000d). In the first step, wind speed at the hub height of the wind turbine is estimated by the following equation.

$$V_{HUB} = V_A \frac{\ln \left(\frac{H_{HUB}}{H_0} \right)}{\ln \left(\frac{H_A}{H_0} \right)} \quad (15)$$

where, V_{HUB} , V_A , H_{HUB} , H_0 , and H_A refer to wind speed at the hub height of the wind turbine (ms⁻¹), speed of wind at the anemometer height (ms⁻¹), wind turbine hub height (m), surface roughness length (m), and anemometer height (m), respectively.

In the second step, turbine power is calculated at standard air density, and it is done by using the turbine power curve given by manufacturers. Wind speed at the hub height is used to calculate the output power in this step.

The third step deals with the correction of air density. By using Eq. (16), actual wind power is calculated by correcting the density.

$$P_{ACTUAL} = \left(\frac{\rho}{\rho_0} \right) P_{STP} \quad (16)$$

Table 4
GPS and annual average solar radiation in five ports.

Port name	GPS	Annual average solar radiation (kWh/m ² /d)
Al Basrah Oil Terminal (Iraq)	30.5590579/47.7900577	5.09
Ain Shukna (Egypt)	29.5856193/32.4612422	5.69
Sidi Kirayr (Egypt)	31.0310915/29.6033959	5.87
Rotterdam Maashaven (Netherlands)	51.8983638/4.4811579	2.81
Pulau Bukom (Singapore)	1.2338147/103.7603323	4.56

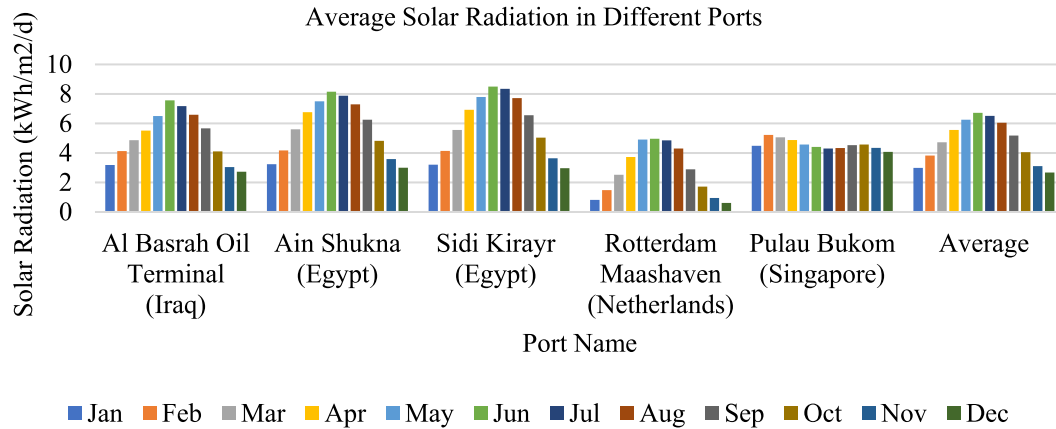


Fig. 6. The average monthly solar radiation in five ports on the shipping route along with the average solar radiation of all five ports.

where, P_{ACTUAL} , ρ , ρ_0 , and P_{STP} denote wind turbine actual power output (kW), actual air density (kg/m³), air density at standard temperature and pressure (kg/m³), and wind turbine power output at standard temperature and pressure (kW), respectively. The parameters of the wind turbine are summarized in Table 5.

The monthly average wind speed of five ports along with the average wind speed of all five ports is presented in Fig. 7.

2.6. MR/SMR

The initial cost of conventional NPPs is very high, and it needs a large area to be installed. Therefore, conventional NPPs are not appropriate if the power requirement is low (Morales Pedraza, 2017). SMRs and Micro Reactors (MRs) are innovative solutions to reduce the high initial cost of NPPs and to eliminate the requirement of a large installation area.

International Atomic Energy Agency (IAEA) refers to 'Small' NPP if the power rating is below 300 MWe and 'Medium' NPP if the power rating is up to 700 MWe. Both types of NPP are termed as 'Small and Medium Reactor (SMR)', but in general, they are called 'Small Modular Reactor (SMR)' (Anon, 0000f). SMRs are getting more attention over conventional NPPs as they can satisfy the requirement of flexible power generation for different applications. SMRs are factory fabricated in a controlled environment, it has a simple design and inherent safety features, and flexible transportation options. As it has modular feature, multiple units can be installed if demand rises.

SMRs can easily replace the decommissioned coal-fired power plants. 90% of the coal-fired plant is rated as less than 500 MWe, and some of these plants are under 50 MWe (Anon, 0000f). Currently, more than 50 SMR designs are under process for different applications, where 6 of them are marine-based. Industrial demonstration of 3 SMRs is ongoing, and they are expected to be in service within 2022 (Anon, 2018a). Small scale reactors producing around 1 MWe to 50 MWe can be termed as Microreactors (MRs), and it can be transported by semi tractor-trailers (Anon, 2020g).

Assessment of the feasibility of MRs for the military ground application was studied in Allen et al. (2018). This study concluded that MRs are better option compared to diesel generators

considering strategical complication, inherent risk, and associated cost for using diesel generator in 'Forward Base Operation'. In collaboration with the US military, HolosGen is working on designing an MR. This MR is configurable to supply from 3 MWe to 81 MWe with load-following operation. The MR could fit into an ISO standard shipping container (40 ft). It uses 8% to 15% enriched TRISO fuel, and the refueling interval is 12 to 20 years (Filippone and Jordan, 0000).

From MR, there are no GHG emissions during operation. However, if fossil fuel is used during the refining or mining of uranium ore, there will be GHG emissions, which is not considered in this study. The first deployment cost of any new technology is likely to be higher compared to the consecutive deployment since the cost can be reduced by experience gained and lesson learning. Hence, the capital cost of MRs is not linear. It is expected that the capital cost of MRs will be reduced with the increment of MR units. By using Eq. (17), the capital cost of multiple MR units can be calculated (Gabbar et al., 2020a).

$$MR_{\text{cap}} = \sum_{i=1}^{N_{\text{MR}}} MR_{\text{cap}(1st)} \times (N_{\text{MR}})^R \quad (17)$$

where, MR_{cap} , $MR_{\text{cap}(1st)}$, N_{MR} , and R refer to the total capital cost of the MR (\$), the first unit deployment cost of the MR unit (\$), number of MR units required, and rate of cost reduction (%) per doubling of units, respectively. The rate of cost reduction is reported as 10% to 20% (Anon, 0000g). The value of R is negative, and the value of R is considered as 15% in this study. The parameters of MR are summarized in Table 6.

2.7. Energy storage

Lithium-ion battery cells are considered in this study as ESS. The lifetime of the battery is 10 years (Anon, 0000a). SOC_{\max} and SOC_{\min} are 100% and 30%, respectively. The capital cost and replacement cost of the battery at the system-level are 500 USD/kW (Anon, 0000a). The efficiency of the battery is considered as 85%. System-level cost includes the cost of the battery cell, insulation cost, and cooling system cost.

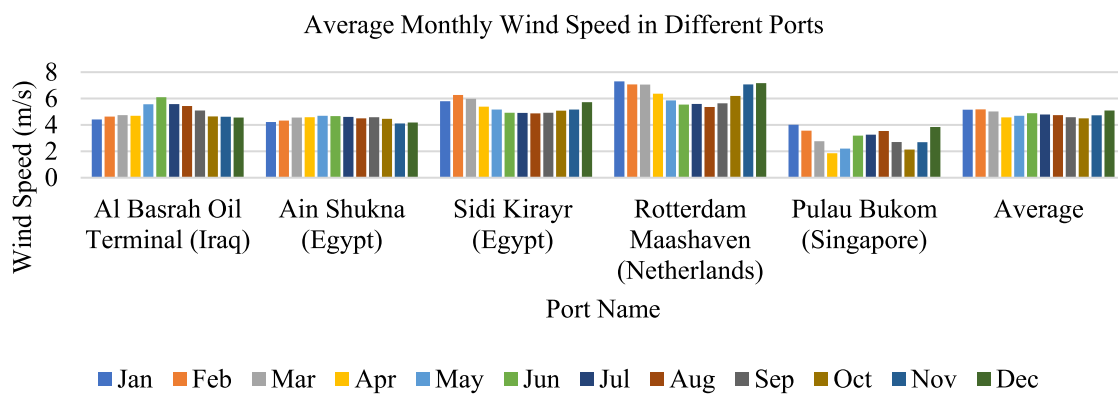


Fig. 7. The average monthly wind speed in five ports on the shipping route along with the average wind speed of all five ports.

Table 5
Specification of some system equipment.

Parameters	System equipment		
	Solar PV	Wind turbine	FFG (Gabbar et al., 2020)
Nominal capacity (kW)	1	10	1000
Capital cost (USD)	640 (Gabbar et al., 2020)	13,000 (Anon, 0000e)	300,000
Replacement cost (USD)	640 (Gabbar et al., 2020)	13,000	200,000
Lifetime (Years)	30 (Gabbar et al., 2020)	20 (Gabbar et al., 2020)	2.5
Operation and maintenance cost (USD/year)	0	400 (Mirzaei and Vahidi, 0000)	87,600

Table 6
Specification of the MR.

Parameter	Value
Fuel type	Uranium
Nominal capacity (kW)	1000
Capital cost (USD/kW)	15,000,000 (Gabbar et al., 2020a)
Operation and maintenance cost (USD/lifetime)	1,510,000 (Abram et al., 2011)
Lifetime (Years)	40 (Anon, 0000f)
Efficiency (%)	40 (Abram et al., 2011)
Fuel Price (USD/kg)	1390 (Anon, 0000h)
Refueling cost (USD)	20,000,000 (Gabbar et al., 2020a)
Core lifespan (Years)	10 (Gabbar et al., 2020a)
Refurbishment cost (USD)	2,300,000 (Gabbar et al., 2020)

3. Design considerations

To assess the techno-economic feasibility of this N-R HES for marine ships, three most influential KPIs are considered in this study, namely NPC, COE, and GHG Emissions. Also, fuel price, expenses, and efficiency of equipment would not be fixed for the entire project life. A multi-year analysis is conducted to address this variability that affects the considered KPIs.

3.1. Key performance indicators

3.1.1. Net present cost

The Net Present Cost (NPC), also termed as Life-Cycle Cost, is the present value of all costs including installing and operating costs over the project lifetime, minus the present value of all revenue earned by the components over the project lifetime. In HOMER, the NPC of each system component is calculated to determine the system NPC (Anon, 0000i).

Eqs. (18)–(19) can be used to calculate NPC. However, NPV and NPC differ only in sign.

$$\text{Net Present Cost (NPC)} = -\text{Net Present Value (NPV)} \quad (18)$$

$$\text{NPV} = \frac{\text{Cash flow}}{(1+i)^t} - \text{Initial Investment} \quad (19)$$

where, i and t denote discount rate (%) and time periods number, respectively.

To calculate the NPC for a longer project lifetime with multiple cash flows, the formula can be modified as follows.

$$\text{NPV} = \sum_{t=0}^n \frac{R_t}{(1+i)^t} \quad (20)$$

where, R_t and n refer to net cash inflow-outflow in a unit time period, and project lifetime, respectively.

3.1.2. Cost of energy

The COE is the average cost per unit of useful electrical energy, kilowatt-hour (kWh). COE can be calculated from the following equation (Anon, 0000j).

$$\text{COE} = \frac{C_{\text{ANNUAL, TOTAL}} - C_{\text{BOILER}} H_{\text{SERVED}}}{E_{\text{SERVED}}} \quad (21)$$

where, E_{SERVED} , H_{SERVED} , C_{BOILER} , and $C_{\text{ANNUAL, TOTAL}}$ refer to total electrical load served annually (kWh/year), total thermal load served annually (kWh/year), the marginal cost of a boiler (\$/kWh), and the total annual cost of the system (\$/year), respectively. As thermal load is not considered in this study, this formula can be simplified as follows.

$$\text{COE} = \frac{C_{\text{ANNUAL, TOTAL}}}{E_{\text{SERVED}}} \quad (22)$$

3.1.3. Greenhouse Gas emissions

Pollutants are emitted from generators due to electricity generation. Pollutants that are normally emitted from generators are Carbon Monoxide, Particulate matter, Nitrogen Oxides, Carbon Dioxide, Sulfur Dioxide, and Unburned Hydrocarbons (UHC).

The annual emissions from a generator are calculated from the below equation (Gabbar et al., 2020).

$$E_{\text{gen}} = E_{\text{factor}} \times T_{\text{fuel}} \quad (23)$$

where, E_{gen} refers to the emissions of any pollutant by generators, E_{factor} is the emissions factor (9) amount of pollutant emits per unit fuel consumption), and T_{fuel} is the total fuel consumption by the generators.

Table 7

Parameters of multi-year analysis.

Criteria	Value (change in %/year)
PV degradation	0.4 (Gambone, 2020)
Fuel price increment (Uranium)	0.0257 (Anon, 2018b)
Fuel price increment (Diesel)	10 (Gabbar et al., 2020)

In HOMER, emissions of six pollutants can be calculated, namely Carbon Monoxide (CO), Particulate matter (PM), Nitrogen Oxides (NO_x), Carbon Dioxide (CO₂), Sulfur Dioxide (SO₂), and Unburned Hydrocarbons (UHC). In HOMER, the emission factor can be specified for all pollutants except Carbon Dioxide (CO₂) and Sulfur Dioxide (SO₂). By using the following three principle assumptions, HOMER calculates the emissions of Carbon Dioxide (CO₂) and Sulfur Dioxide (SO₂). Firstly, any carbon in the fuel that is not emitted as carbon monoxide or unburned hydrocarbons is emitted as carbon dioxide. Secondly, the carbon fraction of the UHC emissions is the same as that of the fuel. Lastly, any sulfur in the burned fuel that is not emitted as particulate matter is emitted as sulfur dioxide.

In HOMER, emissions penalty for pollutants is considered in other O&M costs, and it is calculated by the following equation (Anon, 0000k).

$$C_{\text{om},\text{other}} = C_{\text{om},\text{fixed}} + C_{\text{cs}} + C_{\text{emissions}} \quad (24)$$

where, $C_{\text{om},\text{other}}$ is the other operation and maintenance cost (\$/year), $C_{\text{om},\text{fixed}}$ is the system equipment operation and maintenance cost (\$/year), C_{cs} is the cost for capacity shortage (\$/year), and $C_{\text{emissions}}$ is the penalty for pollutants emissions (\$/year). As there is no capacity shortage considered in this study, the value of C_{cs} is zero.

The following equation is used in HOMER to calculate the penalty for emitting pollutants.

$$C_{\text{emissions}} = \frac{C_{\text{CO}_2} M_{\text{CO}_2} + C_{\text{CO}} M_{\text{CO}} + C_{\text{UHC}} M_{\text{UHC}} + C_{\text{PM}} M_{\text{PM}} + C_{\text{SO}_2} M_{\text{SO}_2} + C_{\text{NO}_2} M_{\text{NO}_2}}{1000} \quad (25)$$

In this study, only the CO₂ emissions penalty is considered. Around 40 national governments and 20 sub-national governments introduced carbon pricing till 2015. Among these national and sub-national governments, 15 have explicit carbon taxes. Fig. 8 shows the tax rate on CO₂ emissions (Farid et al., 0000).

Although nation wise carbon tax varies a lot, IMF calculated a large CO₂ emitter countries should be charged between 50 USD/ton to 100 USD/ton by 2030 to fulfill their commitments to lessen the carbon emissions (Parry, 2021). For the shipping industry, IMF proposed 30 USD/ton CO₂ as penalty for emissions (Anon, 2020h). In this study, 30 USD/ ton CO₂ is considered as CO₂ emissions penalty to show the impact on NPC and COE.

3.2. Multi-year analysis

A multi-year analysis is performed in this study to address the variability of the parameters that affect the KPIs of economic analysis. In the multi-year analysis, three parameters are considered that are PV panel efficiency degradation, uranium price increment, and diesel price increment. The change of the parameters in each year is summarized in Table 7.

3.3. Control algorithm

The control strategy is shown in Fig. 9. Firstly, available resources are assessed, and then load assessment is taken place. The control algorithm is divided into two parts. The control algorithm

inside the green border refers to the algorithm of the supervisory controller and the algorithm inside the blue border refers to the algorithm of the low-level controller. This Hierarchical control strategy was used by Garcia et al. (2015) for Nuclear Hybrid Energy Systems (NHES) Configuration. The supervisory controller dynamically identifies the electrical load and the required electrical energy delivery to the load with the help of the operation optimizer and renewable energy generation profile. Based on the information of the supervisory controller, the low-level controllers change the parameters accordingly.

The load demand $P_L(t)$ updates in each time step based on the load profile and the energy resources can be calculated by the following equation

$$P_{\text{gen}}(t) = P_{\text{pv}}(t) + P_w(t) + P_{\text{MR}}(t) \quad (26)$$

where, $P_{\text{gen}}(t)$, $P_{\text{pv}}(t)$, $P_w(t)$, and $P_{\text{MR}}(t)$ refer to the total energy generation, total energy from solar PV, total energy from the wind turbine, and total energy from MR at time step t , respectively. \

The amount of energy that can be given to the battery and the amount of energy that is needed from the battery bank at any time step can be calculated by the following equations

$$BAT_{\text{in}}(t) = (P_{\text{gen}}(t) - P_L(t)) \times \eta_{\text{bat}}; \quad P_{\text{gen}}(t) > P_L(t) \quad (27)$$

$$BAT_{\text{out}}(t) = \frac{P_L(t) - P_{\text{gen}}(t)}{\eta_{\text{bat}}}; \quad P_{\text{gen}}(t) < P_L(t) \quad (28)$$

where, $BAT_{\text{in}}(t)$ is the amount of energy that can be given to the battery at time step t , $BAT_{\text{out}}(t)$ is the amount of energy that is needed from the battery at time step t , and η_{bat} is the battery efficiency. However, the amount of energy that the battery can give to the system and the amount of energy that can be taken by the battery at any time step depend on the energy status of the previous time step which can be formulated by the below equations

$$BAT_{\text{take}}(t) = BAT_{\text{SOC},\text{max}} - BAT_{\text{e}}(t-1) \quad (29)$$

$$BAT_{\text{give}}(t) = BAT_{\text{e}}(t-1) - BAT_{\text{SOC},\text{min}} \quad (30)$$

where, $BAT_{\text{take}}(t)$ is the amount of energy that can be taken by the battery at time step t , $BAT_{\text{give}}(t)$ is the amount of energy that can be given by the battery at time step t , and $BAT_{\text{e}}(t-1)$ is the amount of battery energy at the time step $(t-1)$.

The charging and discharging of the battery can be formulated by the following equations

$$BAT_{\text{chrg}}(t) = BAT_{\text{SOC},\text{max}};$$

$$P_{\text{gen}}(t) > P_L(t) \& BAT_{\text{in}}(t) \geq BAT_{\text{take}}(t) \quad (31)$$

$$BAT_{\text{chrg}}(t) = BAT_{\text{e}}(t-1) + BAT_{\text{in}}(t);$$

$$P_{\text{gen}}(t) > P_L(t) \& BAT_{\text{in}}(t) < BAT_{\text{take}}(t) \quad (32)$$

$$BAT_{\text{dischrg}}(t) = BAT_{\text{SOC},\text{min}};$$

$$P_{\text{gen}}(t) < P_L(t) \& BAT_{\text{out}}(t) \geq BAT_{\text{give}}(t) \quad (33)$$

$$BAT_{\text{dischrg}}(t) = BAT_{\text{e}}(t-1) - BAT_{\text{out}}(t);$$

$$P_{\text{gen}}(t) < P_L(t) \& BAT_{\text{out}}(t) < BAT_{\text{give}}(t) \quad (34)$$

$$BAT_e(t) = BAT_{\text{e}}(t-1); \quad P_{\text{gen}}(t) = P_L(t) \quad (35)$$

where, $BAT_{\text{chrg}}(t)$ is the capacity of battery after charging, $BAT_{\text{dischrg}}(t)$ is the capacity of battery after discharging and $BAT_e(t)$ is the capacity of the battery when generation and demand are exactly the same, at step t .

In the control algorithm, if the generation is higher than demand, it first charges the battery and after that, excess energy is dumped. Also, when the generation is lower than the demand, it takes energy from the battery and any further energy is taken from the standby generator. The authors motivated to use this control algorithm by Ismail et al. (2015), Gabbar et al. (2020b).

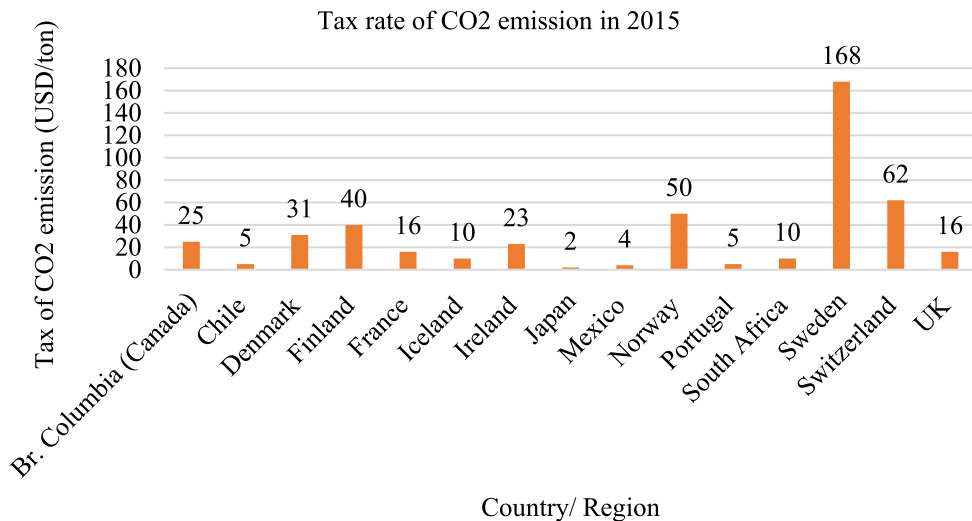


Fig. 8. Tax rate of CO₂ emissions in 2015 (USD/ton CO₂ emissions).

However, to utilize the excess energy and evaluate the impact on the efficiency on the system performance by utilizing the excess energy, flywheel energy storage is employed as shown in Fig. 10. Flywheel stores energy in terms of kinetic energy by braking and accelerating a rotating mass. Flywheel gives operating reserve by absorbing sudden increase or make up sudden decrease in the energy system. The rating of the flywheel is considered 200 kW. The capital cost, replacement cost, O&M cost, and lifetime are 300/kW, 300/kW, 0, and 30 years respectively (Susan and Schoenung, 0000; Sutherland et al., 2021). The impact of adding a flywheel is evaluated in the result section.

The required operating reserve in each time step is regarded as 10% for the electric load. The value of 10% signifies that the studied systems have the capability to serve the demand of a sudden 10% increase. The required operating reserves for PV and solar outputs are 80% and 50%, respectively. The operating reserve of solar PV and WT ensures the system resiliency during a sudden decrease in PV output and WT output. This assumption confirms the utmost reliability of the optimized system.

4. Simulation

Four different types of energy systems are discussed and simulated in this section. HOMER software is used to simulate different types of energy systems. Various components are included in the simulation such as solar power, electric load, wind power, energy storage system, FFG, MR, and power electronics devices.

4.1. Case-01: Stand-alone fossil fuel-based energy system

Conventional fossil fuel-based energy source (diesel generator) along with energy storage system is considered in this case - a common for ocean-going marine ships. There are no renewable energy sources in this case, and this energy system is considered to compare with the proposed N-R HES of marine ships. Fig. 11 represents the system configuration of this case.

Table 8 represents the production of total electricity and consumption by the primary (propulsive and auxiliary) and deferrable load for the first year of project life. As there are no other energy sources other than diesel generator, all electricity is produced by diesel genset. The rating of the diesel generator and battery for this case is 20 MW and 1.6 MW, respectively.

4.2. Case-02: Renewable energy and fossil fuel-based hybrid energy system

In this case, renewable energy sources are integrated with a diesel generator. Parameters of solar and wind energy sources are summarized in Sections 2.4 and 2.5, respectively. Fig. 12 represents the system configuration.

Table 9 summarizes the total electricity production and consumption. In this case, renewable energy penetration is around 5%. Due to the limitation of integrating renewable energy in marine ships, most of the electricity is produced by the diesel generator, which is around 95%. Rating of diesel generator, solar PV, wind turbine, and battery for this case is 20 MW, 1.6 MW, 1.5 MW, and 1.6 MW, respectively.

4.3. Case-03: Stand-alone nuclear energy system

This case is similar to Case-1 except the diesel generator is replaced by the MR. Fig. 13 depicts the system configuration for Case-03.

In this case, MR offers a continuous supply of electricity and total electricity is produced by it. Table 10 shows the total electricity production and consumption in this case. The rating of MR is 20 MWe and the battery rating is 1.6 MW

4.4. Case-04: Nuclear-renewable hybrid energy system (N-R HES)

The integration of nuclear and renewable energy is represented in this case. This case similar to Case-02, where renewable energy is integrated with a diesel generator. The diesel generator of Case-02 is replaced by MR in Case-04. Fig. 14 represents the system configuration.

Most of the electricity is produced by MR in this case that is around 95%. The rest of the electricity is produced by renewable energy sources. The penetration of renewable energy is 5%, where solar energy is 3.63% and wind energy is 1.37%. Ratings of MR, solar PV, wind turbine, and the battery are 19 MWe, 1.6 MW, 1.5 MW, and 1.6 MW, respectively. Table 11 represents the total electricity production and consumption.

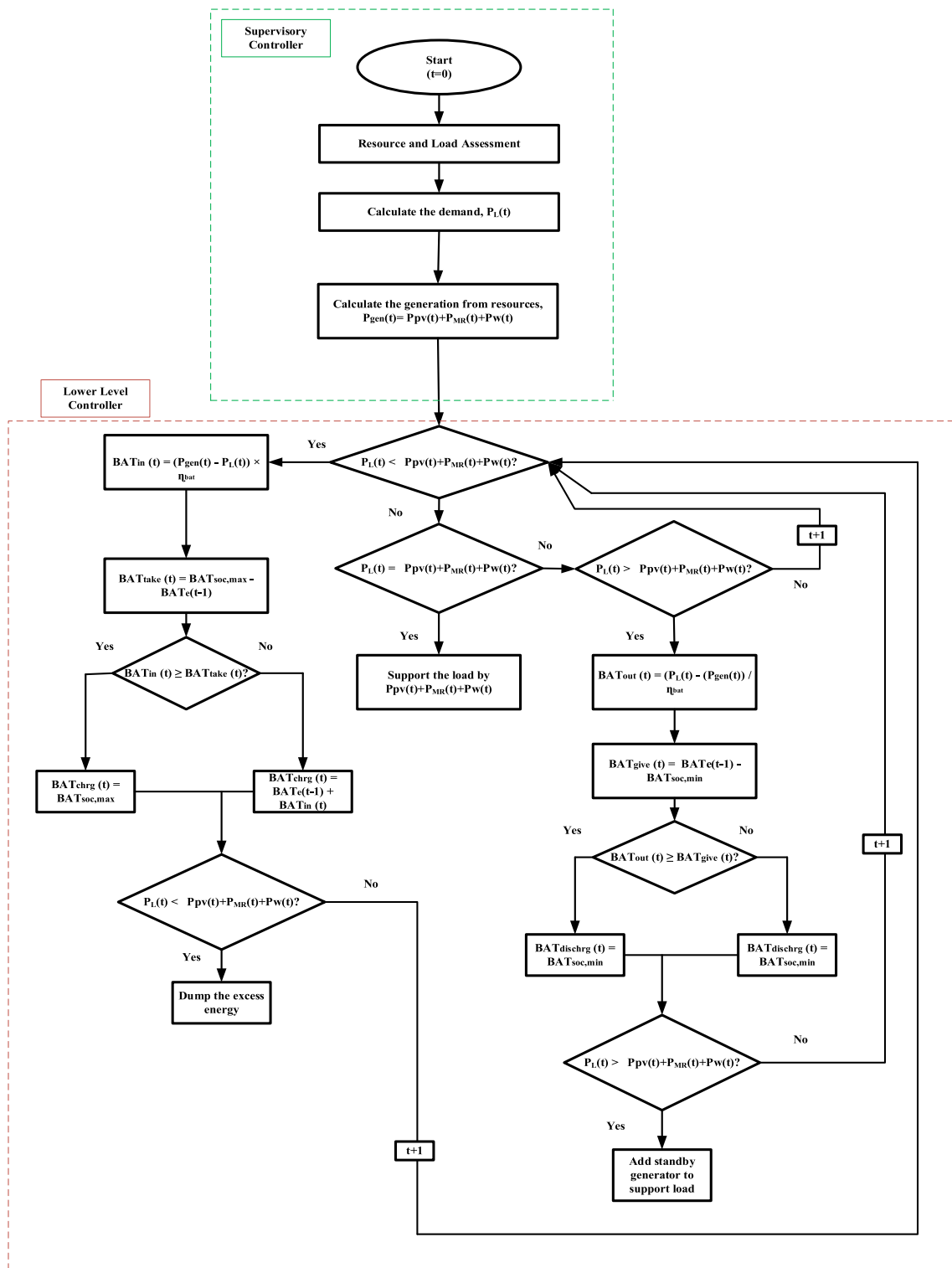
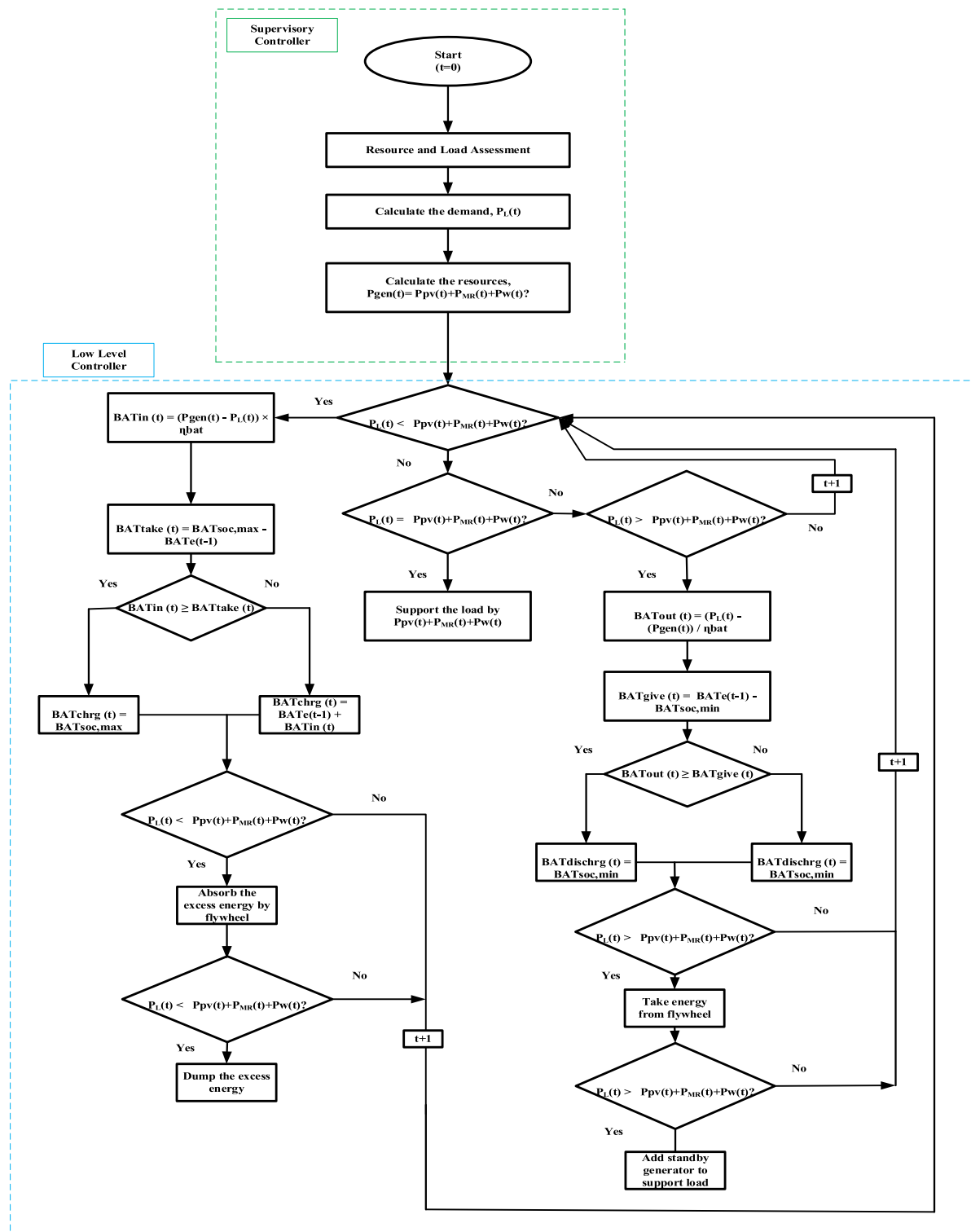


Fig. 9. Control algorithm.. (For interpretation of the references to color in this figure legend, the reader is referred to the web version of this article.)

Table 8

Electricity production and consumption scenario for the first year of project life (Case-01).

Electricity production	Amount (%)	Electricity consumption	Amount (%)
Diesel generator	100	Primary load (propulsive and auxiliary)	95.3
		Deferrable load	4.7
Total	100	Total	100

**Fig. 10.** Control algorithm (excess energy utilization).**Table 9**

Electricity production and consumption scenario for the first year of project life (Case-02).

Electricity production	Amount (%)	Electricity consumption	Amount (%)
Diesel generator	94.8	Primary load (propulsive and auxiliary)	95.3
Wind	1.42	Deferrable load	4.7
Solar	3.78	Total	100
Total	100		

Table 10

Energy production and consumption scenario for the first year of project life (Case-03).

Electricity production	Amount (%)	Electricity consumption	Amount (%)
MR	100	Primary load (propulsive and auxiliary)	95.3
		Deferrable load	4.7

Total 100 Total 100

Table 11

Energy production and consumption scenario for the first year of project life (Case-04).

Electricity production	Amount (%)	Electricity consumption	Amount (%)
MR	95.0	Primary load (propulsive and auxiliary)	95.3
Wind	1.37	Deferrable load	4.7
Solar	3.63	Total	100

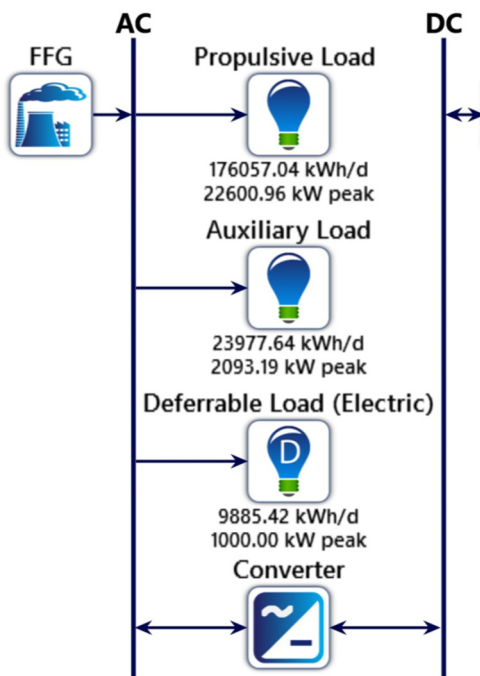


Fig. 11. Stand-alone fossil fuel-based energy system.

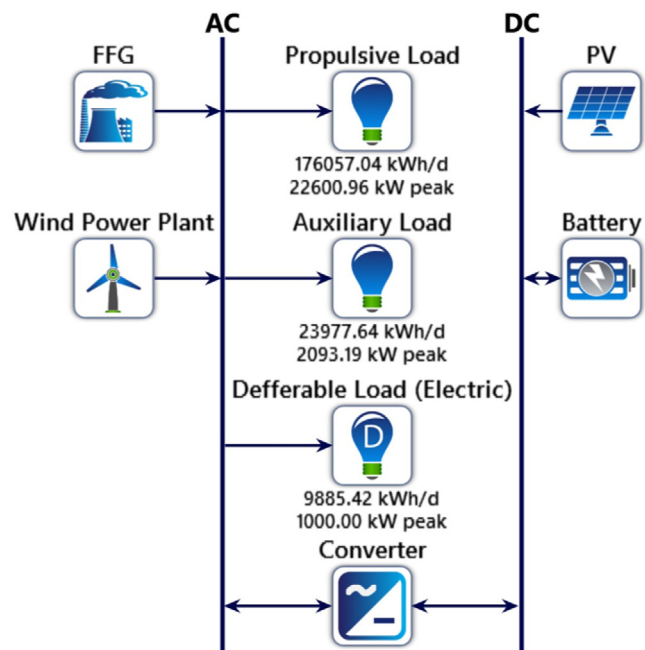


Fig. 12. Renewable energy and fossil fuel-based hybrid energy system.

5. Results

5.1. Comparative analysis among four cases

Three significant KPIs namely NPC, COE, and GHG emissions are studied in this paper. N-R HES is compared with the other three different energy systems based on the three KPIs. NPC and COE of all four cases are shown in Fig. 15.

In terms of NPC and COE, Case-01 exhibits the highest value. For Case-01, NPC is 1,283.47 million USD, and COE is 1.1 USD/kWh. In Case-01, 100% of electricity is produced by the diesel generator, and there is no penetration of renewable energy. Total electricity production in the first year of project life is 81,225,278 kWh. Total fuel consumption is 22,025,144 L in the first year of project life with daily and hourly average fuel consumption are 60,343 L and 2,514 L, respectively.

After integrating renewable energy sources with diesel generator both NPC and COE are reduced to 1,217.57 million USD and 1.04 USD/kWh, respectively in Case-02. Around 5% of electricity is produced from renewable energy. Total electricity production from the diesel generator in the first year of project life for Case-02 is 76,555,746 kWh. In this case, total fuel consumption is

20,765,882 L with daily and hourly average fuel consumption is 56,893 L and 2,371 L, respectively.

Compared to Case-01 and Case-02, the NPC and COE are reduced to a great extent for Case-03 after introducing nuclear energy. In this case, NPC is 276.04 million USD, and COE is 0.236 USD/kWh. In this case, 100% of electricity is produced by MR, and the total electricity production in the first year of project life is 86,053,421 kWh. Total fuel consumption is 794 kg in this case with daily and hourly average fuel consumption are 2.18 kg and 0.0907 kg, respectively.

Case-04 shows the lowest NPC and COE among all the cases. NPC and COE in Case-04 are 271.09 million USD and 0.231 USD/kWh, respectively. The total electricity produced by MR is 80,029,481 kWh whereas solar PV and wind turbine produce 4,192,070 kWh combinedly in the first year of the project lifetime. Due to the integration of renewable energy in Case-04, both NPC and COE are reduced compared to Case-03. Total fuel consumption in the first year for this case is 739 kg. Daily and hourly average fuel consumption are 2.02 kg and 0.0843 kg, respectively.

The decommissioning cost of MR is not considered during the simulation as the impact of the decommissioning cost of MR on the NPC and COE is very low. It will not make any difference in the comparative analysis among the four cases (Anon, 0000g). As the

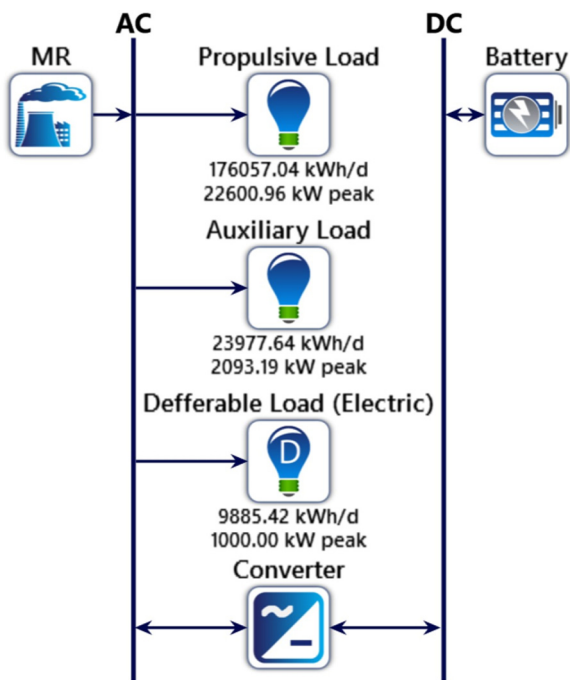


Fig. 13. Stand-alone nuclear energy system.

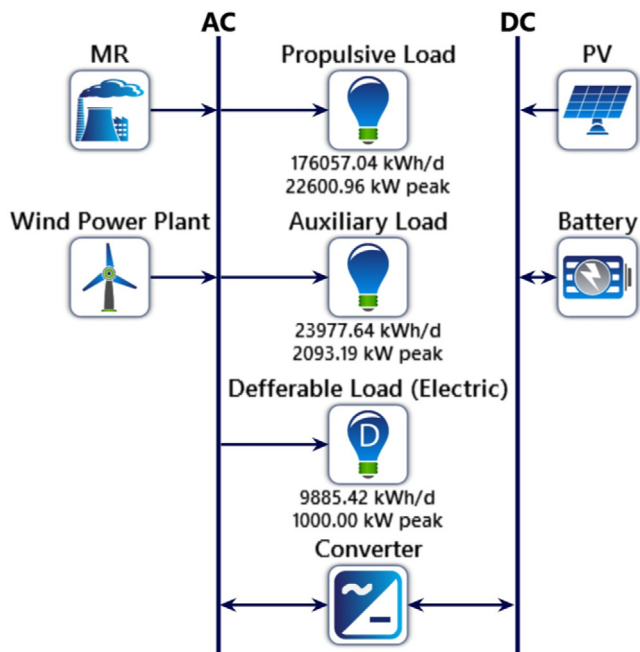


Fig. 14. Nuclear-Renewable Hybrid Energy System (N-R HES).

penetration of RESs in a marine ship is limited due to the available area and the total weight carrying capacity of that marine ship, a standalone RES based energy system is not considered in the simulation. A standalone RES based energy system will not be capable to support the total energy demand of an ocean-going large marine ship (Anon, 2020i).

The weight of the major components of Case-04 needs to be considered if there is any significant impact on the carrying capacity of the ship. In Case-04, the rating of MR is 19 MWe. The weight of 25 MWe SMR is less than 46 MT (Hirdaris et al., 2014). As a conservative assumption, the weight of the 19 MWe

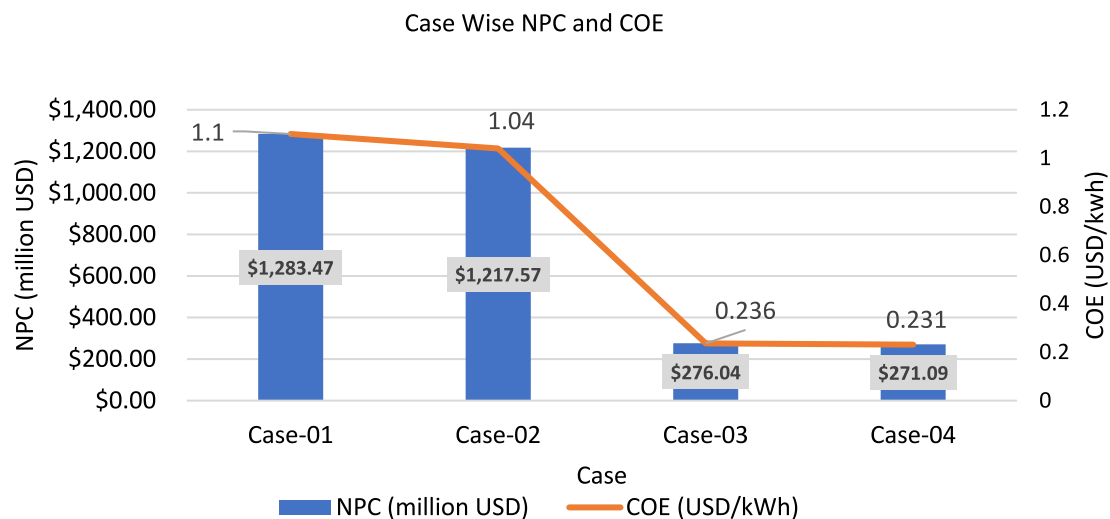
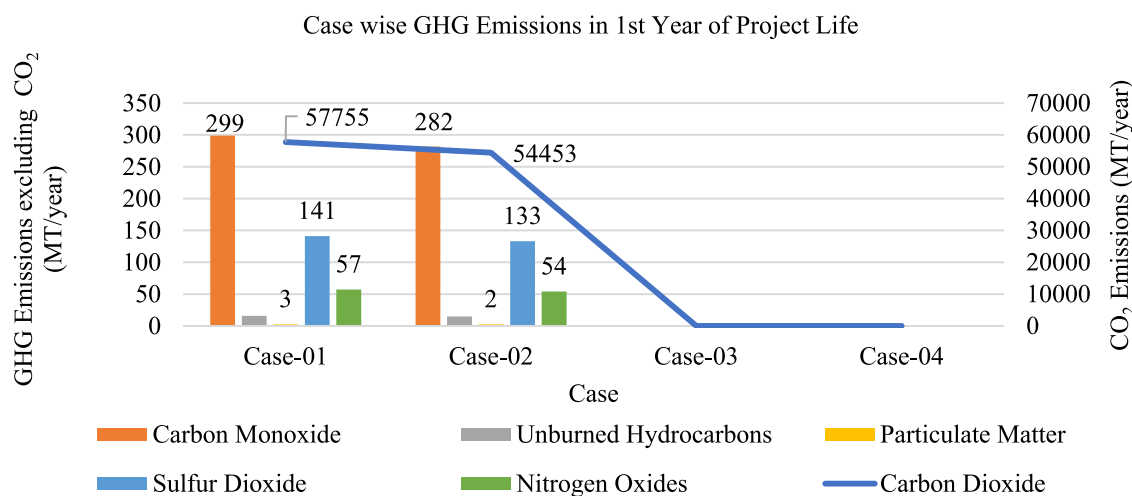
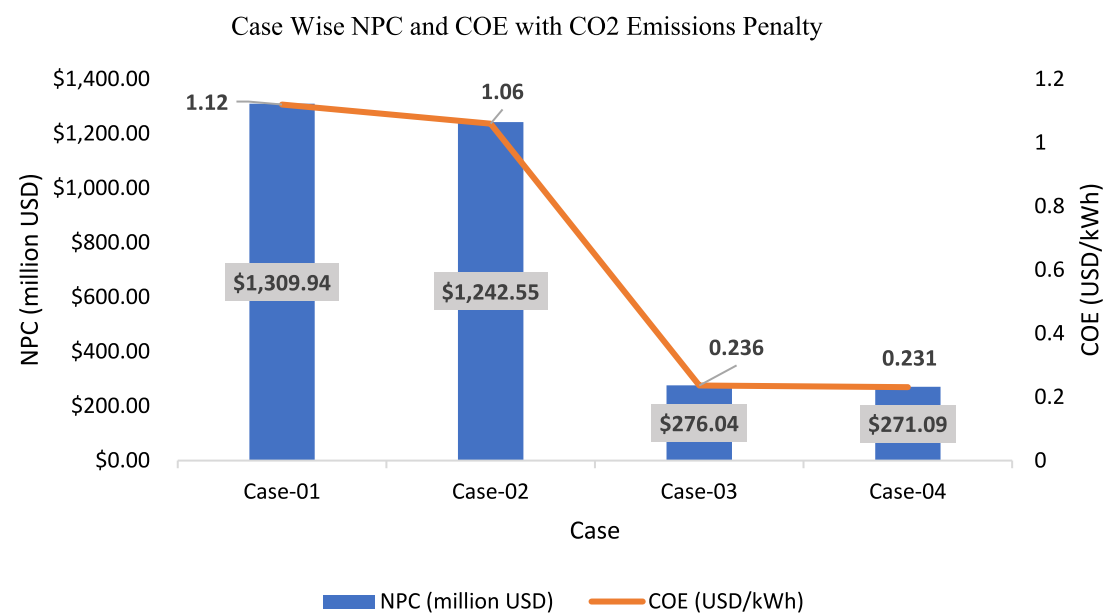
MR is considered as 46 MT. The weight of a full-sized solar panel varies between 40 to 60 pounds. For example, the weight of 'Mission Solar 375 Silver Mono PERC Solar Panel' is 47.6 pounds, which power rating is 375 kW (Anon, 2020j). For 1600 kW solar panel, weight is around 92 MT. The total weight of 1500 kW wind turbine varies from 149 MT to 303 MT considering the weight of nacelle, blade, and tower (Anon, 2020k). In this study weight of the wind turbine is considered as 303 MT. The specific weight of a large (> 1 MWh), heavy-duty marine lithium-ion battery is 30 kg/kWh at system-level including the weight of racks, cooling system, etc. (Anon, 000a). Hence, the weight of 1600 kWh lithium-ion battery is 48 MT but this weight does not include the weight of associated transformers and converters. Therefore, the total weight of the major components of the N-R HES is 489 MT. However, the weight of components varies greatly from manufacturers to manufacturers, and the weight of other minor components is not considered in this calculation. To address these issues, an additional 30% weight is added to the total weight. Hence, the total weight of N-R HES is about 636 MT whereas the total carrying capacity of 'Baltic Sunrise' is 309373 MT (Anon, 2020d). Therefore, the weight of the components of N-R HES is 0.2% of the total weight that the ship can carry with maximum allowable draught.

As this proposed system will replace conventional diesel generator, the weight of the diesel generator needs to be considered to find out the delta amount of weight, which is added to the ship in N-R HES. The weight of ocean-going generator, Sulzer RTA84T (5 cylinders) diesel generator is 672 MT having a power rating of 20.5 MW (Anon, 2020l). Therefore, the total weight of the proposed N-R HES is less than the total weight of a conventional diesel generator implying the proposed system will allow the marine ship to carry more load.

Fig. 16 represents the GHG emissions for all four cases for the first year of the project life. Six types of emissions namely Carbon Monoxide, Carbon Dioxide, UHC, Nitrogen Oxide, Sulfur Dioxide, and Particulate matter are considered in this study. Emissions are considered only for electricity production. GHG emissions for the mining of the fuel (diesel, uranium) and manufacturing of equipment (MR, solar PV, Wind turbine, etc.) are not considered in this study. For Case-01, the highest amount of GHG is emitted. Carbon Dioxide emissions for this case is around 57,755 MT. After introducing renewable energy sources (solar PV and wind turbine) in Case-02, GHG emissions are reduced by around 8%. Carbon Dioxide emissions for this case is around 54,453 MT. As there is no fossil fuel burning in Case-03 and Case-04, there are no GHG emissions.

Fig. 17 shows the NPC and COE of all cases considering the penalty for CO₂ emissions. NPC of Case-01 and Case-02 increases by around 2%, and COE increases by 1.8%. As there are no emissions in Case-03 and Case-04, there is no impact of the CO₂ emissions penalty on NPC and COE for these cases. Hence, it can be inferred that Case-04 will be more feasible considering the CO₂ emissions penalty among all the cases.

As discussed in Section 3.3, to utilize the excess energy, flywheel energy storage is employed to see the performance of different energy systems in terms of NPC and COE. Fig. 18 shows the NPC and COE of different energy systems. Case-04 exhibits the lowest NPC and COE whereas Case-01 shows the highest NPC and COE. However, it is evident that the performance of the system can be improved further by utilizing the excess energy. The NPC of Case-01, Case-02, Case-03, and Case-04 reduce to 1270.73 million USD, 1205.47 million USD, 274.96 million USD, and 270.28 million USD from 1283.47 million USD, 1217.57 million USD, 276.04 million USD, and 271.09 million USD, respectively, by utilizing the excess energy.

**Fig. 15.** Casewise NPC and COE.**Fig. 16.** Casewise GHG emissions (1st year of project life).**Fig. 17.** Casewise NPC and COE with CO₂ emissions penalty.

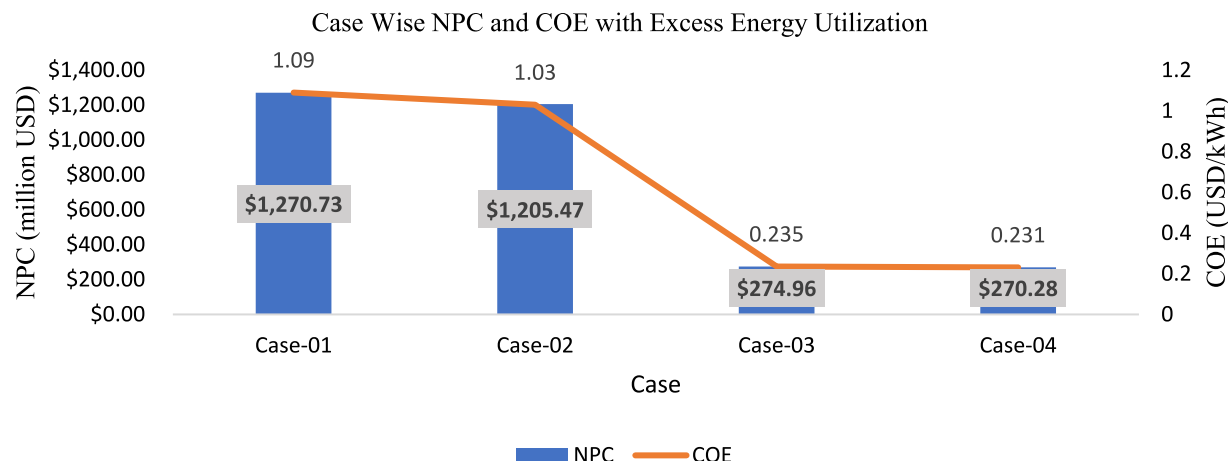


Fig. 18. Casewise NPC and COE with excess energy utilization.

5.2. Sensitivity analysis

Since the analysis depends on several variables, sensitivity analysis is important before providing any concluding remark. In this study, a sensitivity analysis is conducted to identify the impact of four critical parameters – ship power requirement, solar irradiance, wind speed, and penetration of renewable energy. Section 5.2.1 deals with sensitivity to the ship power requirement, and Section 5.2.2 discusses sensitivity to solar irradiance, wind speed, and penetration of renewable energy.

5.2.1. Sensitivity analysis by varying ship power requirement

The estimation of ship power requirement employs several parameters that vary to an extent based on weather, temperature, the position of the ship, and type of ships. Changes in these parameters differ the power requirement of the ship. Hence, it is necessary to conduct a sensitivity analysis to identify the impact of ship power on the performance of the energy systems. In this section, the NPC of the four energy systems has been calculated by varying the ship power requirement from -30% to $+30\%$ with a 10% interval. Fig. 19 summarizes the result of sensitivity to the ship power requirement. The system NPC increases with the increment of ship power requirement. The result shows that Case-04 has the least NPC irrespective of the ship power requirement. The result tells the difference in NPC between Case-03 and Case-04 decreases by lowering the ship power and rises with the increment of ship power.

5.2.2. Sensitivity analysis by varying solar irradiance, wind speed, and penetration of renewable energy

The wind speed and solar irradiance change with the position of the ship in the voyage route. Hence, a sensitivity analysis is carried out for Case-02 and Case-04 by varying the wind speed, solar irradiance, and penetration of the renewable sources. Each parameter value is increased and decreased by 30% in the sensitivity analysis to determine the impact on NPC and COE. As there are no renewable energy sources in Case-01 and Case-03, NPC and COE will not change for these two cases by altering these three parameters. Table 12 represents the result of the sensitivity analysis.

Table 12 indicates that Case-04 is better than Case-01 and Case-02 for all scenarios. If there is no change in the renewable energy penetration, Case-04 exhibits slightly higher NPC and COE compared to Case-03 for lower solar irradiance and wind speed. Scenario No 1, 2, 4, and 7 exemplify this statement. However,

with moderate or high solar irradiance and wind speed, Case-04 has always lower NPC and COE than Case-03, as shown in scenario No 3, 5, 6, 8, and 9.

Despite the 30% increment of renewable energy penetration, Case-04 shows higher NPC and COE than Case-03. This is because of the increased initial cost of renewable energy sources (solar PV and wind turbine), and the absence of enough solar irradiance and wind speed, which is presented in scenario No 10, 13, and 15. However, with moderate or high solar irradiance and wind speed, case-04 has lower NPC and COE, for example, scenario No 11, 12, 14, 15, 17, and 18.

By reducing the percentage of renewable energy by 30%, Case-04 shows higher NPC and COE compared to Case-03, where solar irradiance and wind speed are low or moderate, for instance, scenario No 19, 20, 22, 23, 25, and 26. However, Case-04 shows lower NPC and COE compared to Case-03 for higher availability of solar irradiance and wind speed, for example, scenario No 21, 24, and 27.

This sensitivity analysis tells that Case-04 depicts lower NPC and COE compared to all other cases for moderate and higher availability of renewable resources. However, with the lower availability of renewable resources, Case-04 shows slightly higher NPC and COE compared to Case-03. There are some restrictions on the route for stand-alone nuclear powered marine ships, and a substantial amount of money will be required to get permission to enter into national territorial waters. These issues need to be addressed while comparing Case-04 with Case-03. Sensitivity analysis suggests that the percentage of renewable energy penetration largely depends on the availability of renewable resources that vary based on the route of the marine ship,

6. Conclusion and future works

Several studies have been carried out on stand-alone nuclear energy systems and fossil fuel-renewable hybrid energy systems for ocean-going marine ships to reduce GHG emissions. However, both systems have some limitations, and a nuclear-renewable hybrid energy system on marine ships has been proposed in this paper to overcome these limitations. The findings of this paper suggest that an integrated nuclear-renewable hybrid energy system could be the best solution to make ocean-going ships free from all kinds of emissions, and it is technically and economically feasible. This study also shows that microreactors are a competent candidate to replace fossil fuel-based generators in marine industry.

Impact of Variation in Ship Power Requirement on Different Energy Systems

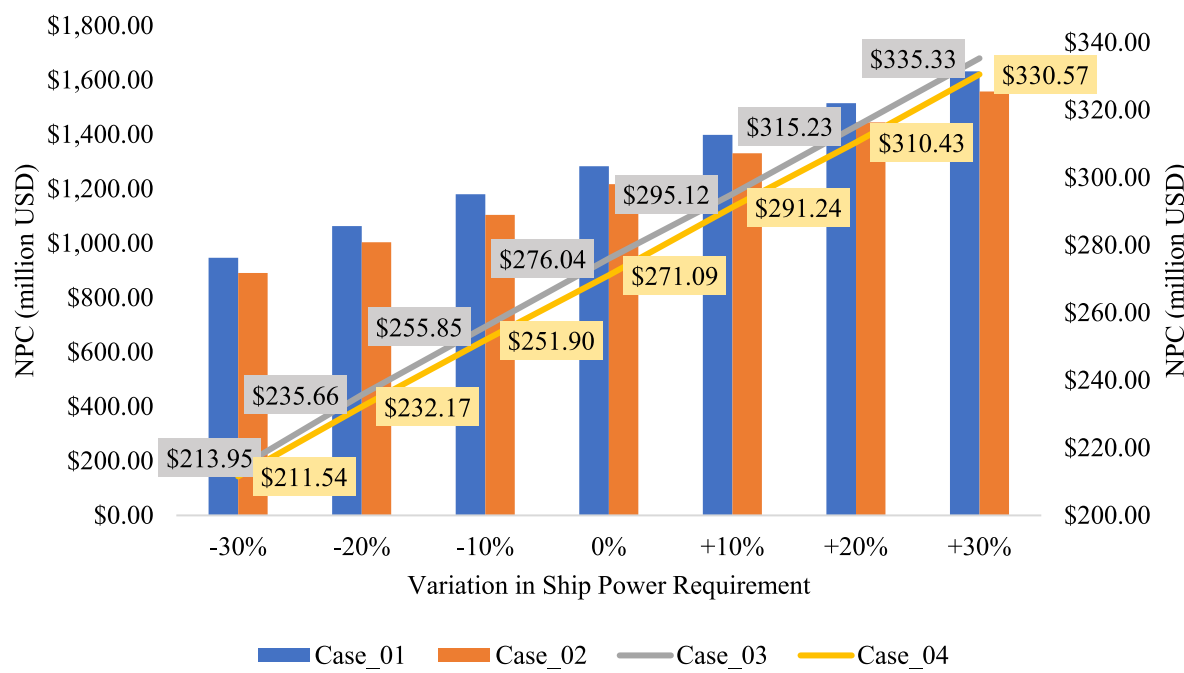


Fig. 19. Impact of Variation in Ship Power Requirement on Different Energy Systems.

Table 12
Sensitivity analysis.

Sl. no.	Renewable energy penetration (solar PV and wind turbine)	Solar irradiance (kWh/m ² /d)	Wind speed (ms ⁻¹)	NPC		COE (USD/kWh)	
				Case-02 (Billion USD)	Case-04 (Million USD)	Case-02	Case-04
1			3.38	1.25	279.22	1.07	0.24
2		3.4	4.83	1.24	279.00	1.06	0.24
3			6.28	1.21	271.06	1.03	0.23
4	No change		3.38	1.23	278.96	1.06	0.24
5		4.8	4.83	1.22	271.09	1.04	0.23
6			6.28	1.19	269.74	1.02	0.23
7			3.38	1.23	278.87	1.05	0.24
8		6.2	4.83	1.21	270.95	1.03	0.23
9			6.28	1.18	269.62	1.01	0.23
10			3.38	1.24	280.46	1.06	0.24
11		3.4	4.83	1.22	272.59	1.04	0.23
12			6.28	1.18	271.12	1.01	0.23
13	30% increased		3.38	1.22	280.13	1.04	0.24
14		4.8	4.83	1.20	272.13	1.02	0.23
15			6.28	1.16	270.73	0.99	0.23
16			3.38	1.21	280.02	1.04	0.24
17		6.2	4.83	1.19	271.99	1.02	0.23
18			6.28	1.16	270.61	0.99	0.23
19			3.38	1.27	279.08	1.08	0.24
20		3.4	4.83	1.25	277.81	1.07	0.24
21			6.28	1.23	270.10	1.05	0.23
22	30% decreased		3.38	1.25	277.80	1.07	0.24
23		4.8	4.83	1.24	277.64	1.06	0.24
24			6.28	1.22	269.84	1.04	0.23
25			3.38	1.25	277.75	1.07	0.24
26		6.2	4.83	1.23	277.58	1.05	0.24
27			6.28	1.21	269.75	1.04	0.23

HOMER optimizer considers a fixed rating of all the system parameters for the project lifetime, which is one of the shortcomings of the HOMER optimizer. HOMER optimizer cannot optimize a system if any of the system parameters change over time. In reality, some of the system parameters may change over time to a varying degree. Hence, the HOMER optimizer gives a quasi-optimal value for each system component. In the future, N-R HESs can be optimized considering all the variables and constraints. As the sensitivity analysis shows that NPC and COE of N-R HES vary based on the route of the marine ship, different sea routes can be analyzed in the future to find out the best route of N-R HESs for marine ships in terms of technical and economical KPIs. Different control strategies can also be assessed in future to evaluate the system performance.

CRediT authorship contribution statement

Hossam A. Gabbar: PI and idea, Model, Validation, Review paper. **Md. Ibrahim Adham:** Write main sections, Analysis, Simulation. **Muhammad R. Abdussami:** Participated in modeling and simulation, Edit, Review paper.

Declaration of competing interest

The authors declare that they have no known competing financial interests or personal relationships that could have appeared to influence the work reported in this paper.

Acknowledgment

This research is funded by NSERC, Canada. Thanks to FleetMon for providing ship information.

References

- Anram, T., Marsden, B., Wickham, T., Ding, M., Kloosterman, J.L., Kooijman, T., Linssen, R., 2011. Design of a U-Batteryfi, Vol. 23. Delft Tech. Univ..
- Allen, K.S., Hartford, S.K., Merkel, G.J., 2018. Feasibility study of a micro modular reactor for military ground applications. *J. Def. Manag.* 8.
- Ang, Joo Hock, Goh, Cindy, Saldivar, Alfredo Alan Flores, Li, Yun, 0000. Energy-Efficient Through-Life Smart Design, Manufacturing and Operation of Ships in an Industry 4.0 Environment. MDPI. <http://dx.doi.org/10.3390/en10050610>.
- Anon, 0000. Batteries on board ocean-going vessels. https://www.manes.com/docs/default-source/marine/tools/batteries-on-board-ocean-going-vessels.pdf?sfvrsn=deaa76b8_12.
- Anon, 0000. Solar panel size guide: how big is A solar panel? <https://www.wholesalesolar.com/blog/solar-panel-size-guide>.
- Anon, 0000. How HOMER calculates the PV array power output. https://www.homerenergy.com/products/pro/docs/latest/how_homer_calculates_the_pv_array_power_output.html.
- Anon, 0000. How HOMER calculates wind turbine power output. https://www.homerenergy.com/products/pro/docs/latest/how_homer_calculates_wind_turbine_power_output.html.
- Anon, 0000. Renewable energy cost analysis - wind power. <https://www.irena.org/publications/2012/jun/Renewable-Energy-Cost-Analysis—Wind-Power>.
- Anon, 0000. World nuclear association. Small nuclear power reactors. <https://www.world-nuclear.org/information-library/nuclear-fuel-cycle/nuclear-power-reactors/small-nuclear-power-reactors.aspx>.
- Anon, 0000. Cost competitiveness of micro-reactors for remote markets. <https://www.nei.org/resources/reports-briefs/cost-competitiveness-micro-reactors-remote-markets>.
- Anon, 0000. Nuclear power economics | nuclear energy costs—world nuclear association. <https://www.world-nuclear.org/information-library/economic-aspects/economics-of-nuclear-power.aspx>.
- Anon, 0000. Net present cost. https://homerenergycom/products/pro/docs/latest/net_present_cost.html.
- Anon, 0000. Levelized cost of energy. https://www.homerenergycom/products/pro/docs/latest/levelized_cost_of_energy.html.
- Anon, 0000. Other operation and maintenance cos. https://www.homerenergy.com/products/pro/docs/latest/other_operation_and_maintenance_cost.html.
- Anon, 2018a. Advances in small modular reactor technology developments a supplement to: IAEA advanced reactors information system (ARIS). Edition.
- Anon, 2018b. 2018 Uranium Marketing Annual Report, Vol. 70. U.S. Department of Energy, Washington, DC, USA.
- Anon, 2020. Low carbon shipping and air pollution control. Available: <http://www.imo.org/en/MediaCentre/HotTopics/GHG/Pages/default.aspx> (accessed on 1 Oct 2020).
- Anon, 2020a. CO₂ emissions from cars: facts and figures (infographics). <https://www.europarl.europa.eu/news/en/headlines/society/20190313STO31218/co2-emissions-from-cars-facts-and-figures-infographics#:~:text=Transport%20is%20responsible%20for%20nearly,2050%20compared%20to%201990%20levels>, (accessed on 1 Oct 2020). (accessed 17 Oct. 2020).
- Anon, 2020b. About fleetmon. <https://www.fleetmon.com/company/our-story/>, (accessed 17 Oct. 2020).
- Anon, 2020c. HOMER optimizer ™, a faster path to finding least-cost microgrid options. <https://microgridnews.com/homer-optimizer-a-faster-path-to-finding-least-cost-microgrid-options/>, (accessed 16 Oct. 2020).
- Anon, 2020d. Auke visser's international super tankers. <http://www.aukevisser.nl/supertankers/VLCC%20T-V/id1147.htm>, (accessed 17 Oct. 2020).
- Anon, 2020e. Voyage analyser DEMO. <https://voyage.vesselfindercom/3a9abdd131b21a2a4f7d6acf52f0d2d2>, (accessed 17 Oct. 2020).
- Anon, 2020f. Diesel price. https://www.globalpetrolprices.com/USA/diesel_prices/, (accessed on 11 Sep 2020).
- Anon, 2020g. Microreactors frequently asked questions | microreactors. <https://inl.gov/trending-topic/microreactors/frequently-asked-questions-microreactors/>, (accessed 25 Dec. 2020).
- Anon, 2020h. IMF calls for carbon tax on ships and planes. (Accessed 17 Oct. 2020). (Online). Available: <https://www.theguardian.com/environment/2016/jan/13/imf-calls-for-carbon-tax-on-ships-and-planes>.
- Anon, 2020i. A marine renewable energy solution for modern ships. <https://www.electricvehiclesresearch.com/articles/4131/a-marine-renewable-energy-solution-for-modern-ships>, (accessed 20 Oct. 2020).
- Anon, 2020j. Canadian solar CS6u-335p silver poly solar panel. <https://www.wholesalesolar.com/1930010/canadian-solar/solar-panels/canadian-solar-cs6u-335p-silver-poly-solar-panel>, (accessed 16 Oct. 2020).
- Anon, 2020k. National wind watch. <https://www.wind-watch.org/faq-size.php>, (accessed 16 Oct. 2020).
- Anon, 2020l. RTA84t. https://pdf.nauticexpo.com/pdf/waertsilae-corporation/rtat24872-12529.html#https://img.nauticexpo.com/pdf/repository_ne/24872/rtat24872-12529_1b.jpg, (accessed 16 Oct. 2020).
- Anon, 2021. ENGR 4011 resistance & propulsion of ships. (Accessed: 06 Mar. 2021). (Online). Available: <https://www.engr.mun.ca/%7Ebveitch/courses/rp/Assignments/ITTC-calculation-procedures-Lab1.pdf>.
- Carlton, J.S., Smart, R., Jenkins, V., 2011. The nuclear propulsion of merchant ships: Aspects of engineering, science, and technology. *Journal of Marine Engineering & Technology* 10 (2), 47–59.
- Chuku, Azubuike John, Ukeh, Michael Edwi, Mkpa, Ante, 2017. Estimation of bare hull resistance of a ropax vessel using the ittc-57 method and gertler series data chart. *wjert* 3 (6), 406–422.
- Diab, Fahd, Lan, Hai, Ali, Salwa, 2016. Novel comparison study between the hybrid renewable energy systems on land and on ship. *Renew. Sustain. Energy Rev.* 63, 452–463.
- Farid, Mai, Keen, Michael, Papaioannou, Michael, Parry, Ian, Pattillo, Catherine, Ter-Martirosyan, Anna, other IMF Staff, 0000. After Paris: fiscal macroeconomic and financial implications of climate change. (Online). Available: <https://www.imf.org/en/Publications/Staff-Discussion-Notes/Issues/2016/12/31/After-Paris-Fiscal-Macroeconomic-and-Financial-Implications-of-Global-Climate-Change-43484>.
- Filippone, C., Jordan, K.A., 0000. The holos reactor: A distributable power generator with transportable subcritical power modules.
- Gabbar, H.A., Abdussami, M.R., Adham, Md. I., 2020. Techno-economic evaluation of interconnected nuclear-renewable micro hybrid energy systems with combined heat and power. *Energies* 13 (7), 1642. <http://dx.doi.org/10.3390/en13071642>.
- Gabbar, H.A., Abdussami, M.R., Adham, M.I., 2020a. Optimal planning of nuclear-renewable micro-hybrid energy system by particle swarm optimization. *IEEE Access* 8, 181049–181073. <http://dx.doi.org/10.1109/ACCESS.2020.3027524>.
- Gabbar, H.A., Abdussami, M.R., Adham, M.I., 2020b. Micro nuclear reactors: Potential replacements for diesel gensets within micro energy grids. *Energies* 13 (19), <http://dx.doi.org/10.3390/en13195172>, Art. no. 19.
- Gambone, Sara, 2020. Solar panel degradation and the lifespan of solar panels. <https://www.paradisesolarenergy.com/blog/solar-panel-degradation-and-the-lifespan-of-solar-panels>, (accessed 16 Oct. 2020).
- Garcia, H.E., et al., 2015. Nuclear Hybrid Energy Systems Regional Studies: West Texas & Northeastern Arizona. Idaho National Lab. (INL, Idaho Falls, ID (United States, <http://dx.doi.org/10.2172/1236837>, INL/EXT-15-34503.
- Gravina, J., Blake, J.I.R., Shenoi, A., Turnock, S.R., Hirdaris, S.E., 2012. Concepts for a modular nuclear powered containership. In: 17th International Conference on Ships and Shipping Research. NAV 2012. Napoli, Italy.
- Helms, Jeremy, 2020. World's 15 biggest ships create more pollution than all the cars in the world. (Accessed 17 Oct. 2020). (Online). Available: <https://www.industrytap.com/worlds-15-biggest-ships-create-more-pollution-than-all-the-cars-in-the-world/8182>.

- Hirdaris, S.E., Cheng, Y.F., Shallcross, P., Bonafoux, J., Carlson, D., Prince, B., Sarris, G.A., 2014. Considerations on the potential use of nuclear small modular reactor (SMR) technology for merchant marine propulsion. *Ocean Eng.* 79, 101–130.
- Ismail, M.S., Moghavvemi, M., Mahlia, T.M.I., Muttaqi, K.M., Moghavvemi, S., 2015. Effective utilization of excess energy in standalone hybrid renewable energy systems for improving comfort ability and reducing cost of energy: A review and analysis. *Renew. Sustain. Energy Rev.* 4, 726–734. <http://dx.doi.org/10.1016/j.rser.2014.10.051>.
- JACOBS, J.G.C.C., 2007. Nuclear Short Sea Shipping. M.Sc. Delft University of Technology.
- Lan, Hai, Wen, Shuli, Hong, Ying-Yi, Yu, David C., Zhang, Lijun, 2015. Optimal sizing of hybrid PV/diesel/battery in ship power system. *Appl. Energy* 158, 26–34. <http://dx.doi.org/10.1016/j.apenergy.2015.08.031>.
- Mirzaei, M., Vahidi, B., 0000. Feasibility analysis and optimal planning of renewable energy systems for industrial loads of a dairy factory in Tehran, Iran. <http://dx.doi.org/10.1063/1.4936591>.
- Molland, Anthony F., Turnock, Stephen R., Hudson, Dominic A., 0000. Ship Resistance and Propulsion, PRACTICAL ESTIMATION OF SHIP PROPULSIVE POWER. p. 207 (Chapter 10).
- Morales Pedraza, J., 2017. Small Modular Reactors for Electricity Generation. Springer, Cham, Switzerland.
- Parry, Ian, 2021. Countries are signing up for sizeable carbon prices. <https://blogs.imf.org/2016/04/21/countries-are-signing-up-for-sizeable-carbon-prices/#more-12399>, (accessed 06 Jan. 2021).
- Paulson, Midhu, Chacko, Dr. Mariamma, 2019. Marine photovoltaics: A review of research and developments, challenges and future trends.. *International Journal of Scientific & Technology Research* 8 (09).
- Perera, Lokukaluge P., Mo, Brage, Kristjánsson, Leifur A., 2015. Identification of optimal trim configurations to improve energy efficiency in ships. *IFAC* 48 (16), 267–272. <http://dx.doi.org/10.1016/j.ifacol.2015.10.291>.
- Qiu, Yuanchao, Yuan, Chengqing, Tang, Jinrui, Tang, Xujing, 0000. Techno-economic analysis of PV systems integrated into ship power grid: A case study. <https://doi.org/10.1016/j.enconman.2019.111925>.
- Shipping Pollution, 2020. OCEANA protecting the world's ocean. <https://europe.oceana.org/en/shipping-pollution-1>, (accessed 17 Oct. 2020).
- Susan, Dr., Schoenung, M., 0000. Overview of energy storage cost analysis. (Online). Available: https://www.google.com/search?q=Overview+of+Energy+Storage+Cost+Analysis+Pre-Conference+Workshop+Houston%2C+TX&safe=active&sxsrf=ALEKk02CS-k-C1K3HiW8_1xXJBGrUSUBlg%3A1617955003648&ei=uwhwYICKJ9a3tQa13q-4DQ&oq=Overview+of+Energy+Storage+Cost+Analysis+Pre-Conference+Workshop+Houston%2C+TX&gs_lcp=Cgdnd3Mtd2l6EAM6BwgjEOoCECdQ4boNWOG6DWDXwA1oAXACeACAfwBiAHUA5IBAzItMpgBAKABAaABAqoBB2d3cy13aXqwAQrAAQE&scrlt=gws-wiz&ved=0ahUKEwjA04SK2PDvAhXWW80KHTXvC9cQ4dUDCA0&uact=5#.
- Sutherland, Will, Senesky, Matthew, Ph.D, Kwok, Wei-Tai, Stout, Mark, Sanders, Seth, PhD, Chiao, Ed, 2021. Flywheel systems for utility scale energy storage. (Accessed: 09 Apr. 2021) (Online). Available: <https://www.energy.gov/2019publications/CEC-500-2019-012/CEC-500-2019-012.pdf>.
- Wen, Shuli, Lan, Hai, Dai, Jinfeng, Hong, Ying-Yi, Yu, David C., Yu, Lijun, 2017. Economic analysis of hybrid wind/PV/Diesel/ESS system on a large oil tanker. *Electric Power Components and Systems* 45 (7), 705–714. <http://dx.doi.org/10.1080/15325008.2017.1292569>.